

## Consistent three-nucleon forces in the nuclear many-body problem

P. Grangé,<sup>(a)</sup> A. Lejeune,<sup>(b)</sup> M. Martzloff,<sup>(c)</sup> and J.-F. Mathiot<sup>(d)</sup>

<sup>(a)</sup>*Institut Laue Langevin, F-38042 Grenoble CEDEX, France*

<sup>(b)</sup>*Université de Liège, Institut de Physique au Sart-Tilman B.5, B-4001 Liège 1, Belgium*

<sup>(c)</sup>*Centre de Recherche Nucléaire, F-67037 Strasbourg, France*

<sup>(d)</sup>*Institut de Physique Nucléaire, Division de Physique Théorique, F-91406 Orsay CEDEX, France*

(Received 2 November 1988)

Describing an assembly of an infinite number of nucleons in interaction via a two-body potential as a nonrelativistic many-body problem in the first place, we envisage corrections to this picture due to suppressed degrees of freedom at the level of the two-body potential. At variance with relativistic many-body theory, the solution of the nonrelativistic problem with a two-body potential only is sufficiently under control at present so that evaluating corrections in this framework is of particular interest. These corrections come primarily from additional three-body forces either due to finite-density effects (Pauli blocking of fermions) or are of genuine origin: relativistic dynamical processes and effects from the intrinsic structure of the nucleon. Recalling the successful treatment of electromagnetic interactions in nuclei in terms of meson-exchange currents, we establish novel consistency requirements between the initial two-body force and the well-identified residual three-body force. In this way no new parameters enter in the three-body force, save for the controversial mass of the fictitious scalar " $\sigma$ " meson. We show further that the nucleon-antinucleon pair term required in the analysis of meson-exchange currents has a genuine three-body counterpart resulting from time-ordered diagrams containing a single  $Z$  branch. Its contribution to the energy per particle is repulsive and varies with a high power of the density. Thereby we obtain the important saturating effect present in relativistic mean-field approaches. We envisage next the role of the first radial nucleon resonance  $N^*(\frac{1}{2}, \frac{1}{2})$  (Roper resonance) in inducing a specific three-body force. The meson-nucleon-Roper coupling constants and form factors are evaluated in a relativistic quark model. Gathering all self-consistent corrections to the binding energy per particle of infinitely many nucleons, we find that the final equation of state is solely governed by the density dependence of medium corrections to the free  $\sigma$ -meson mass. We discuss a first attempt to extract this density dependence from an empirical equation of state.

### I. INTRODUCTION

Relativistic effects in atomic nuclei have long been looked at to interpret certain of their observed properties. Besides the early case of the spin-orbit coupling,<sup>1</sup> the successful reproduction of spin observables, at first glance a traditional shortcoming of simple nonrelativistic calculations, is commonly and cheerfully ascribed to the use of relativistic nuclear dynamics. Cross section, analyzing power, and the angular dependence of the spin rotation parameter are often given as "good" examples in this respect.<sup>2</sup>

Among the numerous pending questions in nuclear physics one of the most basic and constantly addressed is that of the binding of nuclei and infinite nuclear matter. It is a highly nontrivial problem as an unambiguous answer in terms of the mechanism of saturation can only be given after a reliable treatment of the nuclear many-body problem itself. In the nonrelativistic approach, where the interaction between nucleons is modeled via two-body potentials, it took about thirty years to come to the conclusion that the nuclear many-body problem is well under control by different techniques.<sup>3-5</sup> The important outcome is now a wide recognition that in this nonrelativistic framework the mechanism of saturation of

the nuclear medium cannot be understood in terms of a two-body potential only, whatever its ability in reproducing two-body observables.

Even before the "success" of Dirac phenomenology, the whole question of saturation has been investigated in relativistic mean field<sup>6,7</sup> and Brueckner-Hartree-Fock type calculations.<sup>8-10</sup> It is found that genuine saturating effects appear,<sup>11</sup> which are associated with the negative energy solutions of the Dirac equation for the fermion field. However, the knowledge, on the one hand, of the structure and treatment of negative energy components of the nucleon and, on the other hand, of the convergence properties of the relativistic many-body problem and relevance of mean-field approximations in that respect, are rather elusive. Nevertheless, it is often argued that the various approximations made there find de facto, their justifications for the empirical properties of nuclear matter *emerge without throes*. Clearly, considering the present status of the relativistic many-body problem, this cannot be so.<sup>12</sup>

What remains as an important effect arising from the relativistic approach is a repulsive contribution in the energy per particle which varies with a high power of the density and is instrumental for saturation. It occurs, due to strong excitation of nucleon-antinucleon pairs ( $Z$

graphs) by the meson field. Before considering these processes in more detail we would like to present first what is our general philosophy with respect to relativistic corrections in nuclear physics.

Up to an energy scale at which the internal baryon structure is resolved, a relativistic description of nuclear systems from an effective Lagrangian with interacting mesons and baryons may be relevant. This, however, requires some justification. First of all, the use of such Yukawa-type models valid at all distances cannot be legitimated,<sup>13</sup> as often advocated. Despite the existence of renormalizable perturbative expansion in simplified cases of effective Lagrangians, a cutoff independent theory is only guaranteed by an approach to the continuum with scaling properties as in the case of quantum chromodynamics. In fact, the intrinsic and unremovable cutoff<sup>13</sup> of such effective field theories is of the order of one to two times the nucleon mass. Hence, it may be altogether tenable to seek a relativistic description of nuclear physics phenomena in terms of mesons and baryons degrees of freedom only below this energy scale, where common relativistic expansions may be used further.

In lowest order in a  $p/M$  expansion, the excitation of a nucleon-antinucleon pair from a scalar interaction is proportional to the momentum of the nucleon, and therefore vanishes when the nucleon is at rest, as it should. Such a transition already occurs in meson-exchange currents<sup>14</sup> (pair terms) for the part of the current associated with the spin-orbit potential. These contributions are required by the conservation of the electromagnetic current. As a consequence, and apart from straightforward vertex factors, the same form factor should be used at the meson-nucleon and meson-antinucleon vertices, for small three-momentum transfer. This is in fact the case in the Hartree approximation, and in the Hartree-Fock approximation, the momentum transfer is still much smaller than, e.g.,  $1 \text{ GeV}/c$ .

One can equivalently interpret these dynamical relativistic contributions as Pauli corrections to the free meson mass (cf., Sec. III), since this latter includes implicitly all polarization effects, such as polarization of the Dirac sea from meson exchange.<sup>15</sup> Translated in terms of a quark model for the nucleon structure, this effect may be related to the calculation of the Casimir energy contribution<sup>16</sup> to the nucleon mass in the presence of other nucleons. In this sense, one may doubt that a simple perturbative approach of the nucleon structure in terms of valence quarks only is relevant to understanding these relativistic contributions.

However, it is rather easy to realize that this description of the nuclear dynamics cannot be complete, because the nucleon has a structure and therefore excited states must be considered at the same time. In fact, since nucleon-antinucleon excitations are taken into account, one should also include all states up to an excitation energy of about  $1.8 \text{ GeV}$ . This can be done implicitly in any quark model by coupling mesons to the individual quarks, but also at the level of the physical states, if one knows the various coupling strengths.

In this study we shall consider an (infinite) ensemble of nucleons as a nonrelativistic many-body problem. Its

solution is under reasonable quantitative control with respect to convergence properties. Hence, it is of particular interest to study corrections in this framework. It is well known that the two-body potential between nucleons appears because mesonic degrees of freedom have been suppressed from the nuclear wave function. Furthermore, due to Pauli blocking, the two-meson exchange part of the nucleon-nucleon ( $NN$ ) potential is modified in the medium. This gives rise to many-body forces, and in first order in the hierarchy, to three-body forces (see Fig. 1). Traditional three-body forces (3BF) are associated with  $\pi$ - and  $\rho$ -exchange and are well documented.<sup>17-21</sup> Likewise, the relativistic nucleon-antinucleon corrections associated with  $\sigma$ - and  $\omega$ -exchange give rise to three-body forces which in the nonrelativistic limit do not disappear and at finite density should embody the dominant relativistic saturating features.<sup>11-22</sup>

Considering these corrections from the three-body diagrams, we would have gained little in terms of a consistent picture between the initial two-body and residual three-body nucleon interaction if we let the coupling constants, meson masses, and hadronic form factors evolve freely, and take on values suited to reproduce the empirical nuclear matter properties. Our next concern is the possibility and importance of these consistency requirements. We shall emphasize that this is possible to a large extent from the actual knowledge of meson-exchange current (MEC) operators. Current conservation between the isovector current and the  $NN$  potential, here the Paris potential,<sup>23</sup> and consistency between the isoscalar part of the Paris spin-orbit potential and the one-boson-exchange (OBE) approximation with  $\sigma$ - and  $\omega$ -exchange fix all the model parameters, except for the mass of the scalar meson. As the three-body forces contributions are in keeping with this analysis of  $NN$  potential and MEC's, they imply no new parameters. This will be the content of Sec. II.

In Sec. III our purpose will be to construct a three-nucleon potential from time-ordered diagrams containing a single  $Z$  branch which occur mainly through exchange of scalar  $\sigma$ - and  $\omega$ -mesons. In this procedure, we shall see the importance of keeping contributions of same order in the expansion in terms of momenta over the nucleon mass  $M$ , not only those involving momentum transfer but also those involving individual momenta of nucleons. It is this very dependence which brings the genuine saturating effect observed in relativistic calculations.<sup>6-12,22</sup>

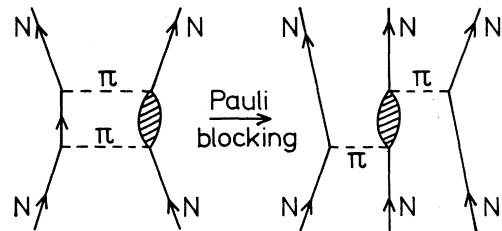


FIG. 1. In medium Pauli blocking of the intermediate nucleon and the single exchange  $2\pi$  three-body force.

The 3BF being fixed in a manner consistent with the use of the two-body interaction, we want next to check the conjecture on the saturation mechanism induced in nuclear matter by  $\sigma$ - and  $\omega$ -meson contributions with one  $Z$  branch. For that purpose we need a reliable and well studied treatment of the nuclear matter many-body problem. Variational calculations have proved very successful in this context.<sup>4,5,22,24</sup> Here we shall perform a nonrelativistic Brueckner-Bethe calculation which includes the effect of the 3BF via the introduction of an additional effective two-body interaction. This line of approach has been used in the past<sup>17-19</sup> and in the case of the Paris potential, shown to give results<sup>4,25</sup> in essential agreement with those obtained through alternative techniques. The treatment of three-body forces through the introduction of an effective two-body force results from the formalism of McKellar and Rajaraman.<sup>26</sup> However, tensor correlations in the nucleon state summed over to generate the effective two-body force as well as double exchange contributions are not considered. Nevertheless it offers the interesting possibility of generating perturbative direct and single exchange contributions without solving the full three-body problem. They are obtained from the self-consistent solution of the Bethe-Goldstone integral equation involving the bare two-nucleon potential (Paris potential) plus this effective two-body potential. Treating the three-body force this way, we shall show that its basic saturating features are taken into account properly. Hence, the saturation trends we obtain in our nonrelativistic nuclear matter calculations are reliable. These developments and results will form the content of Sec. IV.

Our last question arises about the possible role of nuclear resonances in inducing a specific 3BF when considering the exchange of a scalar meson, as in the previous section. We remark first that the Roper resonance, being only 200 MeV above the  $\Delta$  isobar, cannot be disregarded solely on the basis of arguments on energy denominators. Moreover, the Roper has the same quantum numbers as the nucleon, at variance with the spin  $\frac{3}{2}$  Isobar. It can thus easily couple spins with surrounding nucleons, thereby possibly boosting its effects despite its expected small coupling constants and specific form factors. In Sec. V we consider the derivation of the  $(\sigma, \omega)$ -exchange three-body force mediated by the Roper resonance. We shall evaluate the meson-nucleon-Roper coupling constants and form factors from a relativistic model—the color dielectric model<sup>27</sup>—in which the nucleon has a bag-like structure. This will permit fixing the  $\sigma$ - $\omega$  exchange 3BF via the Roper and evaluating its contribution in nuclear matter in the same approach as in Sec. IV. In the last section a concluding discussion is presented.

Sticking to the description of nuclear systems in terms of mesons and nucleons, we think that the perturbative approach presented in this work is a satisfactory way to reconcile the intrinsic structure of the nucleon with dynamical relativistic effects inherent to such a description. This approach is in keeping with the successful treatment of electromagnetic interaction in nuclei in terms of meson-exchange currents. However, a consistent calculation can only be achieved when the whole set of baryonic excitations in the nuclear wave function is

considered. This goal is certainly very difficult to achieve given our limited knowledge of coupling constants between meson, nucleon, and nucleon resonances. We present in the following a first attempt in such a coherent description of nuclear systems.

## II. CONSISTENCY REQUIREMENTS BETWEEN TWO- AND THREE-BODY FORCES

### A. Three-body forces and meson-exchange currents

In the OBE description of the  $NN$  interaction, an effective Lagrangian density is constructed from various mesonic degrees of freedom generally identified as two isovector mesons, the pion ( $\pi$ ) and the rho ( $\rho$ ), and two isoscalar mesons the sigma ( $\sigma$ ) and omega ( $\omega$ ). The pion field has long been identified from peripheral  $N$ - $N$  scattering and deuteron data as the source of the long range part of the  $NN$  potential, while the  $\rho$  meson is responsible for the spin-isospin symmetry properties of the nuclear medium. The  $\omega$ -meson vector field is also well identified and gives rise to a strong short-range repulsion accounting for the observed behavior of the scattering phase shift in the singlet  $S$  state above 250 MeV. The  $\sigma$  meson provides attraction at intermediate range on a purely empirical basis. Its interpretation and the fundamental understanding of this intermediate range attraction has been at the heart of investigations on the  $NN$  force for more than two decades. We shall comment on this question in the sequel.

The derivation of a consistent three-body force cannot be disentangled in any way from the two-body  $NN$  potential one starts from. This can be very easily visualized if one recalls that 3BF are just Pauli corrections in the medium ( $A > 3$ ) to the two-meson exchange part of the  $NN$  potential. We illustrate this point in Fig. 1, where for simplicity we restrict ourselves to the  $2\pi$  exchange potential. For the part which involves a nucleon in the intermediate state [Fig. 1(a)], Pauli blocking will restrict the possible states and therefore the  $NN$  potential must be corrected accordingly. This is done by considering the correction indicated in Fig. 1(b), a pure 3BF contribution. The dashed blob in this figure involves many different contributions which we shall discuss later on. They contribute to the  $\pi N$  scattering amplitude.

The consistency requirements between two- and three-body forces is rather easy to achieve in the OBE description of the  $NN$  potential. Here we prefer to use the Paris potential derived directly from dispersion relations for the most important long- and medium-range part. The foremost reason is that it includes the exact mass distribution of the  $2\pi$  exchange system, either in the  $P$  channel ( $\rho$  meson), or in the  $S$ -channel ( $\sigma$  meson). As we shall see below, this leads to rather important deviations from the simple parametrization in terms of single (zero-width) mesons. The short-range part is purely phenomenological, contrarily to OBE potentials for which the structure of the potential is taken the same at all distances. This may explain why the  $p^2$  dependent part of the Paris potential is much more important in this region than in the OBE potentials.

The price to pay for the use of the Paris potential is that the ensuing form of the 3BF is not obvious. To find it, it is necessary to disentangle from the parametrization of the potential the different channels associated with specific meson exchange. This can be done rather easily with the use of MEC's and the requirement of current conservation. Starting from a given  $NN$  potential, the conservation of the total electromagnetic current  $\mathbf{J}$  writes, in the nonrelativistic limit for an energy-independent potential

$$\nabla \cdot \mathbf{J} + i[H, \rho] = 0, \tag{1}$$

where

$$H = T + V_{NN}. \tag{2}$$

In Eq. (2),  $T$  is the nonrelativistic kinetic energy and  $V_{NN}$  the two-body potential. If one decomposes the charge density ( $\rho$ ) and current ( $\mathbf{J}$ ) operators in their one- and two-body parts

$$\begin{aligned} \mathbf{J} &= \mathbf{J}^{(1)} + \mathbf{J}^{(2)}, \\ \rho &= \rho^{(1)} + \rho^{(2)}, \end{aligned} \tag{3}$$

the continuity equation can be rewritten in the following form

$$\begin{aligned} \nabla \cdot \mathbf{J}^{(1)} + i[T, \rho^{(1)}] &= 0, \\ \nabla \cdot \mathbf{J}^{(2)} + i[V_{NN}, \rho^{(2)}] &= 0, \end{aligned} \tag{4}$$

where we neglect here three-body exchange currents and small contributions from  $[T, \rho^{(2)}]$ . If the  $NN$  potential is now interpreted in terms of meson exchange, it is easy to identify the elementary processes in  $\mathbf{J}^{(2)}$ . We indicate in Fig. 2(a) the various MEC's which contribute to Eqs. (4) in leading order. The first two diagrams are associated with the isospin-dependent part of the  $NN$  potential (mainly tensor potential for  $\pi$  and  $\rho$  exchange) while the

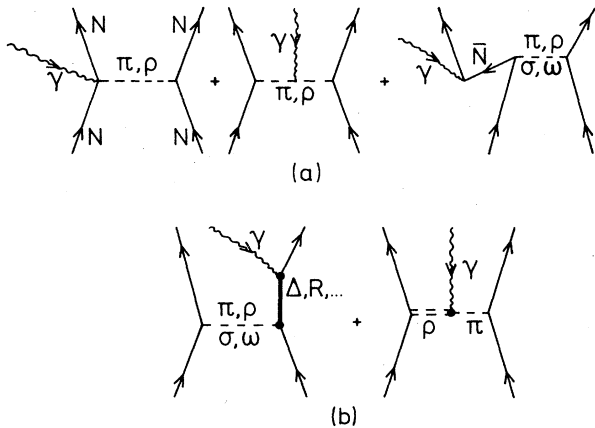


FIG. 2. (a) Leading MEC contributions constrained by the continuity equation. From left to right: seagull, mesonic, and pairs diagrams. (b) Gauge invariant contributions to MEC's in first order: contribution from nucleon resonances and  $\rho\pi\gamma$  diagram.

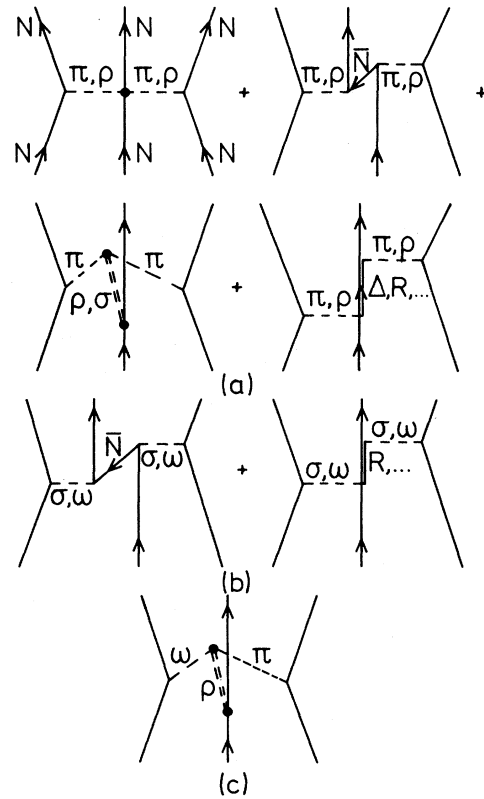


FIG. 3. Leading order contributions to the three-body force deduced from the meson-exchange current operators indicated in Fig. 2. See text for the explanation of the various groups (a)–(c).

third diagram comes from the spin-orbit part of the potential (associated with  $\sigma$  and  $\omega$  exchange in the OBE approximation). We recall in Fig. 2(b) the two other leading order contributions to MEC's which are gauge invariant by themselves and hence do not contribute to Eqs. (4). They are associated to nucleon excitations and the  $\rho$  decay into  $\pi\gamma$ .

The relationship between MEC's and 3BF contributions can be understood as follows. If one replaces the external currents (vector current here associated with the photon, or axial current for weak interactions), by meson lines coupled to a third nucleon, one can generate all contributions to the 3BF in leading order (two-meson lines) with no additional parameters. The corresponding contributions are indicated in Fig. 3. They have been separated in three different groups for the purpose of the discussion. As one can realize immediately from Eq. (4), this procedure fixes only the longitudinal part of the current, and, moreover, it concerns the leading order contribution associated with a given  $NN$  potential, and does not fix higher-order corrections. This is however, sufficient to determine all the parameters entering the elementary processes, once these have been identified in terms of the degrees of freedom we start from, as given in Figs. 2 and 3.

### B. Determination of the parameters

The 3BF contributions of Fig. 3(a) have already been derived, at low momentum transfer, from  $\pi N$  scattering amplitude in both  $S$  and  $P$  channels, and extended to include  $\rho\rho$  and  $\pi\rho$  exchange as well.<sup>18</sup> Therefore, they include all the contributions indicated by a dashed area in Fig. 1, and are consistent with the Paris potential derivation for the  $2\pi$ -exchange part. The parameters which have to be given are the masses, coupling constants, and form factors at the meson-nucleon vertices. According to our discussion of the preceding subsection, we have determined these quantities by comparing MEC's (here isovector currents) associated with the Paris potential from Eqs. (4), to MEC's derived in the OBE approximation, and represented in Fig. 3. By looking at the radial distribution of the corresponding operators, it is possible to fix all these parameters.<sup>14</sup> We summarize these quantities in Table I. The form factor at each meson-nucleon vertex is chosen in a monopole form

$$F(q^2) = \frac{\Lambda^2 - m^2}{\Lambda^2 - q^2} \xrightarrow{q_0 \approx 0} \frac{\Lambda^2 - m^2}{\Lambda^2 + q^2}, \quad (5)$$

where  $m$  is the meson mass and  $\Lambda$  a cutoff parameter (different *a priori* for each meson).

For  $\rho$  exchange, we have to fix various quantities since the  $2\pi$  amplitude in the  $\rho$ -channel is rather broad. As a consequence, the range of MEC's associated to this part of the potential is larger than for a single  $\rho$  exchange with the physical mass  $m_\rho = 776$  MeV. With the parameters indicated in Table I, the tensor part of the  $NN$  potential is given in Fig. 4 (small dashed line), and compared with the exact Paris tensor potential. The two potentials agree together to a very large extent. In particular, the behavior of the tensor potential at distances smaller than 0.5 fm agrees with that of the Paris potential, while the parametrization of Refs. 17 and 18, using a zero-width approximation for the  $\rho$  meson gives a positive tensor potential in this domain.

The 3BF corrections indicated in Fig. 3(b) are associated with  $\sigma$  and  $\omega$  exchange in the OBE approximation. They have not yet been considered in detail so far. We shall discuss the calculation of the second contribution in Sec. V. The first one is derived directly from the MEC diagrams shown in Fig. 2(a) (pair term) and therefore the

TABLE I. Coupling constants and form factors at the different vertices. The meson masses are  $m_\pi = 138$  MeV,  $m_\omega = 783$  MeV and  $m_\sigma = 540$  MeV,  $m_\rho = 600$  MeV (see text for discussion). The tensor to vector coupling constant ratio for the  $\rho$ -meson is  $\kappa_\rho = 5.6$  (Ref. 14).

	$g^2/4\pi$	$\Lambda$ (GeV/c)	$\alpha$
$\sigma NN$	11.9	1.1	
$\omega NN$	33	1.3	
$\pi NN$	14.4	1.4	
$\rho NN$	0.55	1.1	
$\sigma NR$	2.58	1.45	-2.35
$\omega NR$	4.13	1.55	-2.33

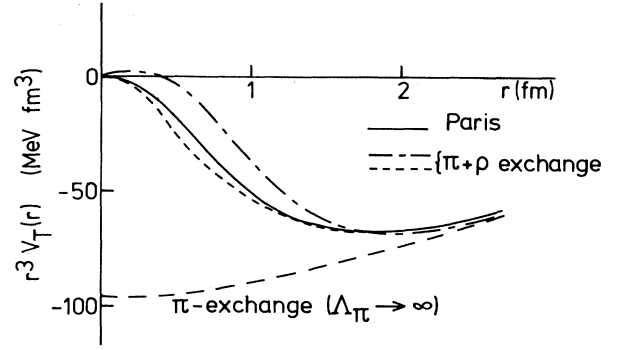


FIG. 4. The nucleon-nucleon tensor potential as function of relative internucleon distance. Dashed line:  $\pi$ -exchange contribution with no form factors; dash-dotted line:  $\pi$ - and  $\rho$ -exchange contributions with form factors and coupling constants of Refs. 17 and 18; continuous line: tensor part of the Paris potential (Ref. 23); short-dashed line:  $\pi$ - and  $\rho$ -exchange contributions with form factors and coupling constants as discussed in the text (see Table I).

various parameters can be fixed from the (isospin independent) spin-orbit part of the  $NN$  potential.

In the cm frame, this part of the potential is expressed in momentum space by

$$V_{LS}(\mathbf{p}', \mathbf{p}) = \frac{i}{2} v(\mathbf{k})(\sigma_1 + \sigma_2)(\mathbf{p}' \times \mathbf{p}), \quad (6)$$

where  $\mathbf{k} = \mathbf{p}' - \mathbf{p}$ . Keeping track of the total momentum of the two nucleons, one has

$$V_{LS}(\mathbf{p}'_1, \mathbf{p}'_2; \mathbf{p}_1, \mathbf{p}_2) = \frac{i}{2} \{ v_a(\mathbf{k})[\sigma_1(\mathbf{p}'_1 \times \mathbf{p}_1) + 1 \leftrightarrow 2] + v_b(\mathbf{k})[\sigma_1(\mathbf{p}'_1 - \mathbf{p}_1) + 1 \leftrightarrow 2] \}. \quad (7)$$

This last expression is necessary to construct MEC's by minimal substitution.<sup>28</sup> In the OBE approximation, the potentials  $v_a(\mathbf{k})$  and  $v_b(\mathbf{k})$  are

$$v_a(\mathbf{k}) = \frac{g_{\sigma N}^2}{2M^2} \frac{1}{m_\sigma^2 + \mathbf{k}^2} F_\sigma(k^2) + \frac{g_{\omega N}^2}{2M^2} \frac{1}{m_\omega^2 + \mathbf{k}^2} F_\omega(k^2), \quad (8a)$$

$$v_b(\mathbf{k}) = \frac{g_{\omega N}^2}{M^2} \frac{1}{m_\omega^2 + \mathbf{k}^2} F_\omega(k^2). \quad (8b)$$

The meson-nucleon coupling constants and the nucleon mass are denoted by  $g_{\sigma N, \omega N}$  and  $M$ , respectively. These potentials can be also derived directly from the Paris potential parametrization.<sup>28</sup> We indicate them in Fig. 5 for both the Paris potential and the OBE approximation with the parameters of Table I. The value at the origin is fixed by the coupling constants, while the momentum-dependence is governed by the mass and form factor. Both parametrizations are in reasonable agreement.

The last point one has to check when going from the two-body system to nuclear matter is the question of the

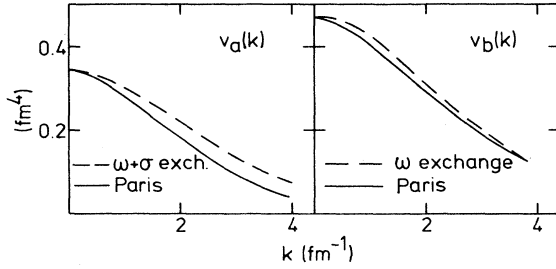


FIG. 5. The spin-orbit potential components  $v_a(k)$  and  $v_b(k)$  of Ref. 28 as obtained from the Paris potential—continuous curve— and for a pure “ $\sigma + \omega$ ” exchange model, Eqs. (8) dashed curve with coupling constants and form factors as indicated in Table I.

density dependence of the various quantities (medium polarization). As far as  $\pi$  and  $\rho$  exchange are concerned, it is easy to realize that the three-body force indicated in Fig. 3(a) corresponds precisely to the polarization of the  $\pi$  and  $\rho$  propagators as well as  $\pi NN$  and  $\rho NN$  vertices in first order, in the nuclear medium. For isovector-meson exchange, these renormalizations are dominated by  $\Delta$ - $h$  excitations. They are indicated, to first order, in Fig. 6. These corrections correspond exactly to the isobar contribution to the 3BF of Fig. 3(a), after summation over the intermediate particle in the Fermi sea. Hence no further modification is needed in this channel.

The situation for  $\sigma$  exchange is much more intricate. Since it is not a well defined resonance, one can expect the  $\sigma$  meson to be strongly polarized in the nuclear medium, the first consequence being a strong modification of its mass as a function of the density. Two mechanisms have been proposed in the literature to account for this change.<sup>29,30</sup> On the one hand, the  $\sigma$  meson, viewed as a  $2\pi$  exchange, has its mass changed in the medium from  $\Delta$ - $h$  excitations in the  $\pi$  line.<sup>29</sup> At normal nuclear matter density, the change may be as large as 20–30%, and leads to a reduction of  $m_\sigma$ . A similar conclusion is reached in the apparently different Nambu-Jona-Lasinio model where the  $\sigma$  meson is taken as the chiral partner of the pion.<sup>30</sup>

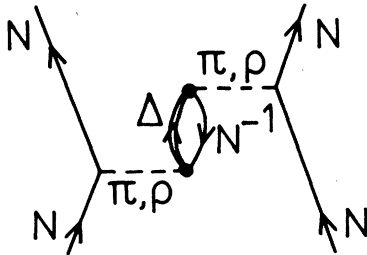


FIG. 6. Polarization of  $\pi$  and  $\rho$  propagators as well as  $\pi NN$  and  $\rho NN$  vertices from  $\Delta$ - $h$  excitations in first order. These corrections are taken into account by the three-body contribution of Fig. 3(a) fourth diagram.

It is certainly too early to draw more quantitative conclusions for the polarization of the  $\sigma$  meson in the nuclear medium. In particular, the  $\sigma NN$  coupling constant may also change. In Ref. 30 this change is found to be very small. In any case, it is likely that the  $\sigma$  mass will be reduced in nuclear matter with respect to its two-body (zero density) estimate of 680 MeV found from Fig. 5(a). This is in fact the only free parameter in our approach, if one assumes that all other mesons keep their free mass and coupling constant. As we shall see in Sec. V, the value of the  $\sigma$  mass cannot be too small, otherwise the saturation properties of nuclear matter are unrealistic. For convenience, we choose here  $m_\sigma = 540$  MeV. We recall that the  $\sigma$  mass deduced from the OBE approximation to the  $NN$  potential can be as large<sup>31</sup> as 720 MeV, depending upon the isospin channel and the detail of the potential. In the relativistic Hartree-Fock description of finite nuclei, a mass of 440 MeV was used.<sup>32</sup>

The last contribution to the 3BF we derived from MEC's is indicated in Fig. 3(c). It originates from the  $\rho\pi\gamma$  diagram of Fig. 2(b) and has never been considered up to now. Because of the isovector  $\pi$  and  $\rho$  exchange, this 3BF contributes only through exchange terms, and therefore should be of smaller importance. This point should however be checked in the future. Note that other three-body contributions involving nonlinear couplings between  $\sigma$  mesons, as originating in the  $\sigma$ -model Lagrangian for instance, have not been retained either since they involve higher order terms not considered in the Lagrangian we start with. We only mention here that these terms cannot be calculated in the tree approximation from the  $\sigma$  model Lagrangian since they give rise to pathological behavior for the nuclear equation of state [3] at moderate densities. Moreover, drastic cancellations occur in the one loop approximation. The resulting contribution to the binding energy is highly sensitive to the  $\sigma$ -meson mass and cannot be settled with accuracy. We restrict ourselves in this study to the 3BF contribution which can be calculated at tree level, and directly connected to the  $NN$  potential itself. We refer the interested reader to Refs. 3 and 11 for an extensive discussion and results concerning this other aspect of the 3BF.

### III. THE SIGMA- AND OMEGA-EXCHANGE THREE-BODY POTENTIAL FROM VIRTUAL PAIR TERMS

The primary feature of recent relativistic mean-field calculations of nuclear properties consists in the “dressing” of the individual nucleon state through the scalar meson-nucleon interaction. The precise mechanism has been analyzed in the past.<sup>7,11,22</sup> We recall it here to stress the underlying 3BF picture of the present perturbative approach.

#### A. Relativistic corrections in effective Lagrangian formulation of nuclear structure

For the purpose of discussing the mechanism which dresses the nucleons, we recall here the simplified model popularized by Walceka<sup>6</sup> which includes only the exchange of the  $\sigma$  and  $\omega$  mesons. The effective Lagrangian writes

$$\begin{aligned} \mathcal{L} = & \bar{\Psi}(i\gamma_\mu\partial^\mu - M)\Psi + \frac{1}{2}(\partial_\mu\sigma\partial^\mu\sigma - m_\sigma^2\sigma^2) \\ & - \frac{1}{4}F_{\mu\nu}F^{\mu\nu} + \frac{1}{2}m_\omega^2\omega_\mu\omega^\mu - g_{\sigma N}\bar{\Psi}\Psi\sigma - g_{\omega N}\bar{\Psi}\gamma_\mu\Psi\omega^\mu, \end{aligned} \quad (9)$$

where  $\Psi$  represents the nucleon field, with mass  $M$ ,  $\sigma$  the scalar meson field, with mass  $m_\sigma$  and  $\omega_\mu$  the vector meson field of mass  $m_\omega$ . In Eq. (9) the regularizing part of the Lagrangian is omitted as it does not enter the discussion. According to the usual notation  $F_{\mu\nu} = \partial_\mu\omega_\nu - \partial_\nu\omega_\mu$ . In translationally invariant nuclear matter the mean field approximation consists in taking for the scalar and vector fields their expectation values over the Fermi sea denoted by  $\langle\sigma\rangle$  and  $\langle\omega_\mu\rangle = \delta_{\mu 0}\langle\omega_0\rangle$ . These quantities are obtained from the field equations

$$\begin{aligned} -m_\sigma^2\langle\sigma\rangle &= g_{\sigma N}\langle\bar{\Psi}\Psi\rangle \\ &= g_{\sigma N}\rho_S \end{aligned} \quad (10a)$$

$$\begin{aligned} m_\omega^2\langle\omega_0\rangle &= g_{\omega N}\langle\bar{\Psi}\gamma_0\Psi\rangle \\ &= g_{\omega N}\rho_B, \end{aligned} \quad (10b)$$

where  $\rho_S$  and  $\rho_B$ , are respectively, the scalar and baryonic densities of the nuclear medium. Defining the scalar and vector self-energies by  $U_S = -g_{\sigma N}^2\rho_S/m_\sigma^2$  and  $U_V = g_{\omega N}^2\rho_B/m_\omega^2$ , the one-body Dirac equation satisfied by the nucleon spinor  $u(\mathbf{p}, \lambda)$  with helicity  $\lambda(\pm 1)$  and energy  $\varepsilon_p$  writes

$$[\boldsymbol{\alpha}\cdot\mathbf{p} + \beta(M + U_S) - (\varepsilon_p - U_V)]u(\mathbf{p}, \lambda) = 0. \quad (11)$$

In this equation characteristic values of the scalar and vector self-energies at a density  $\rho_B$  around the normal density  $\rho_0 = 0.17 \text{ fm}^{-3}$ , are<sup>7</sup>

$$\begin{aligned} U_S &= -400 \left[ \frac{\rho_B}{\rho_0} \right] \text{ MeV}, \\ U_V &= 350 \left[ \frac{\rho_B}{\rho_0} \right] \text{ MeV}. \end{aligned} \quad (12)$$

Let us write

$$\begin{aligned} \bar{\varepsilon}_p &= \varepsilon_p - U_V, \\ \bar{M} &= M + U_S. \end{aligned} \quad (13)$$

The solution of Eq. (11) for  $\bar{\varepsilon}_p$  is that for a quasifree nucleon of effective mass  $\bar{M}$ , momentum  $p = |\mathbf{p}|$ , and helicity  $\lambda$ . It writes

$$u(\mathbf{p}, \lambda) = \left[ \frac{\bar{\varepsilon}_p + \bar{M}}{2\bar{\varepsilon}_p} \right]^{1/2} \begin{bmatrix} 1 \\ \frac{p\lambda}{\bar{\varepsilon}_p + \bar{M}} \end{bmatrix} \chi_\lambda, \quad (14)$$

with  $\bar{\varepsilon}_p^2 = \bar{M}^2 + p^2$ . Let  $u^0(\mathbf{p}, \lambda)$  and  $v^0(\mathbf{p}, \lambda)$  be the spinors with positive and negative energy  $\pm\varepsilon_p^0$  of the free nucleon (no interaction  $U_S = U_V = 0$ ). Then  $u(\mathbf{p}, \lambda)$  may be written identically as<sup>7</sup>

$$\begin{aligned} u(\mathbf{p}, \lambda) = & \frac{1}{2M(\varepsilon_p^0 + M)^{1/2}(\bar{\varepsilon}_p + \bar{M})^{1/2}} \left[ \frac{\varepsilon_p^0}{\bar{\varepsilon}_p} \right]^{1/2} \{ [(\varepsilon_p^0 + M)(\bar{\varepsilon}_p + \bar{M}) - p^2]u^0(\mathbf{p}, \lambda) \\ & + (-1)^{1/2(1-\lambda)}p\lambda[(\varepsilon_p^0 + M) - (\bar{\varepsilon}_p + \bar{M})]v^0(-\mathbf{p}, -\lambda) \}. \end{aligned} \quad (15)$$

This expression shows that the interaction mixes the positive and negative energy components of the free nucleons. To lowest order in  $p^2/M$ , where  $\varepsilon_p^0 = M + O(p^2/M)$ , the change  $\delta u(\mathbf{p}, \lambda)$  of the free spinor  $u^0(\mathbf{p}, \lambda)$  is determined by the difference  $\bar{M} - M = U_S$ . Hence it is the scalar field which gives rise to the first relativistic correction to the propagation of a positive energy single-particle state, as indicated in Fig. 7(a). The corresponding energy correction is represented by Fig. 7(b). It is proportional to  $U_S^2$  and is found simply from relation (15). To lowest order in  $p/M$  it writes<sup>7</sup>

$$\frac{\Delta E}{A} = \rho_B^{-1} \sum_{\lambda, \tau} \int \frac{d^3p}{(2\pi)^3} \theta(k_F - p) \frac{p^2\lambda^2}{2M^3} U_S^2. \quad (16)$$

In this relation  $k_F$  is the Fermi momentum, with  $\rho_B = 2k_F^3/(3\pi^2)$ . Taking for  $U_S$  the value indicated in Eq. (12), summing over isospin and helicity, one obtains<sup>7</sup>

$$\frac{\Delta E}{A} \approx 4.2 \text{ MeV} \left[ \frac{\rho_B}{\rho_0} \right]^{8/3}. \quad (17)$$

This is a strongly saturating quantity genuine to a relativistic framework as antinucleon propagation is not con-

sidered in conventional nonrelativistic approaches to the nuclear many-body problem. Figure 7(a) clearly emphasizes the three-body nature of the scalar coupling to nucleon-antinucleon pairs, while Fig. 7(b) indicates a medium correction to the scalar meson mass  $m_\sigma$ . Both interpretations are equivalent.

### B. The sigma- and omega-exchange 3BF in momentum space

The usual and well documented treatment of three-body forces in the nuclear medium involves<sup>17,18</sup>  $\pi$  and  $\rho$  exchanges between three nucleons. These contributions

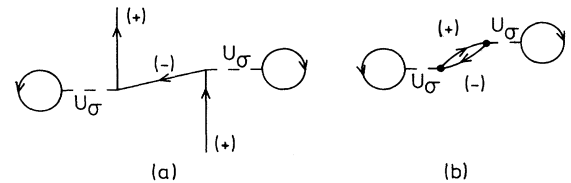


FIG. 7. (a) Relativistic corrections to the propagation of a single nucleon of positive energy. (b) The corresponding contribution to the energy per particle.

help getting closer to the empirical estimate of the binding energy and saturation density of nuclear matter.<sup>17,19,25</sup> Yet these quantities cannot be reproduced without additional phenomenological assumptions.<sup>33,34</sup> Hence, it is legitimate to investigate whether or not the above relativistic corrections treated as additional three-body forces would give a new saturation mechanism in nonrelativistic approaches of the nuclear many-body problem. The question was studied recently both in nuclear matter and in three- and four-body systems<sup>22</sup> within a variational framework. The conclusions however, are only indicative, mainly for two reasons. First the important  $\pi$ - and  $\rho$ -exchange contributions to the 3BF were not included and second, by retaining only those contributions which depend upon the momentum transfer and not upon the individual nucleon momenta in the reduction of the  $Z$  graphs, an essential piece of the saturation mechanism is dropped.

We consider here the general expression for the three-

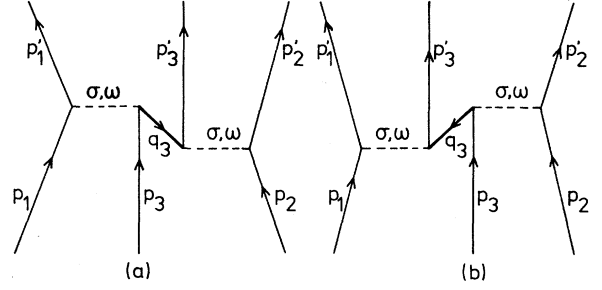


FIG. 8. Backward propagating terms contributing to the two-meson ( $\sigma, \omega$ ) exchange three-body force.

three scattering amplitude  $\langle \mathbf{p}'_1, \mathbf{p}'_2, \mathbf{p}'_3 | T_3 | \mathbf{p}_1, \mathbf{p}_2, \mathbf{p}_3 \rangle$ , with particle 3 undergoing backward propagation. The total amplitude is the sum  $T_1 + T_2 + T_3$ , as is the three-nucleon potential  $W$  defined in terms of the individual  $W_i$  related to  $T_i$  by

$$\langle \mathbf{p}'_1, \mathbf{p}'_2, \mathbf{p}'_3 | W_i | \mathbf{p}_1, \mathbf{p}_2, \mathbf{p}_3 \rangle = (2\pi)^3 \delta^{(3)}(\mathbf{p}'_1 + \mathbf{p}'_2 + \mathbf{p}'_3 - \mathbf{p}_1 - \mathbf{p}_2 - \mathbf{p}_3) N_f N_i \langle \mathbf{p}'_1, \mathbf{p}'_2, \mathbf{p}'_3 | T_i | \mathbf{p}_1, \mathbf{p}_2, \mathbf{p}_3 \rangle. \quad (18)$$

Here  $N_f = \prod_{\nu=1}^3 [M/E(p_\nu)]^{1/2}$ , the index  $\nu$  labeling the particles in the final states (viz: initial states for  $N_i$ ). We adopt throughout the same normalization as in Refs. 17 and 18 and denote the transferred and total momenta by

$$\mathbf{q}_1 = \mathbf{p}_1 - \mathbf{p}'_1, \quad \mathbf{q}_2 = \mathbf{p}_2 - \mathbf{p}'_2, \quad (19)$$

and

$$\mathbf{P}_1 = \frac{\mathbf{p}_1 + \mathbf{p}'_1}{2}, \quad \mathbf{P}_2 = \frac{\mathbf{p}_2 + \mathbf{p}'_2}{2}, \quad (20)$$

respectively.

The time ordered diagrammatic contributions are indicated in Fig. 8 (exchange of  $2\sigma$ ,  $\sigma\omega$ , and  $2\omega$ ). These contributions are calculated in leading order. This corresponds to the static approximation for the meson propagator. To lowest order in  $q^2/m$  we find

$$\begin{aligned} \langle \mathbf{p}'_1, \mathbf{p}'_2, \mathbf{p}'_3 | W_3^{2\sigma} | \mathbf{p}_1, \mathbf{p}_2, \mathbf{p}_3 \rangle &= (2\pi)^3 \delta^{(3)}(\mathbf{p}'_3 - \mathbf{p}_3 - \mathbf{q}_1 - \mathbf{q}_2) \frac{g_{\sigma N}^4}{4M^3} \frac{F_\sigma^2(q_1^2)}{q_1^2 + m_\sigma^2} \frac{F_\sigma^2(q_2^2)}{q_2^2 + m_\sigma^2} \\ &\quad \times [4\mathbf{p}_3^2 + 4\mathbf{p}_3 \cdot (\mathbf{q}_1 + \mathbf{q}_2) + \mathbf{q}_1^2 + \mathbf{q}_2^2 + \mathbf{q}_1 \cdot \mathbf{q}_2 + 2i\boldsymbol{\sigma}_3 \cdot (\mathbf{q}_1 + \mathbf{q}_2) \times \mathbf{p}_3], \end{aligned} \quad (21a)$$

$$\begin{aligned} \langle \mathbf{p}'_1, \mathbf{p}'_2, \mathbf{p}'_3 | W_3^{2\omega} | \mathbf{p}_1, \mathbf{p}_2, \mathbf{p}_3 \rangle &= (2\pi)^3 \delta^{(3)}(\mathbf{p}'_3 - \mathbf{p}_3 - \mathbf{q}_1 - \mathbf{q}_2) \frac{g_{\omega N}^4}{4M^3} \frac{F_\omega^2(q_1^2)}{q_1^2 + m_\omega^2} \frac{F_\omega^2(q_2^2)}{q_2^2 + m_\omega^2} \\ &\quad \times [ -\mathbf{q}_1 \cdot \mathbf{q}_2 - (\boldsymbol{\sigma}_3 \times \mathbf{q}_2) \cdot (\boldsymbol{\sigma}_1 \times \mathbf{q}_1) - (\boldsymbol{\sigma}_3 \times \mathbf{q}_1) \cdot (\boldsymbol{\sigma}_2 \times \mathbf{q}_2) - (\boldsymbol{\sigma}_1 \times \mathbf{q}_1) \cdot (\boldsymbol{\sigma}_2 \times \mathbf{q}_2) \\ &\quad - 2i\mathbf{P}_1 \cdot (\boldsymbol{\sigma}_2 + \boldsymbol{\sigma}_3) \times \mathbf{q}_2 - 2i\mathbf{P}_2 \cdot (\boldsymbol{\sigma}_1 + \boldsymbol{\sigma}_3) \times \mathbf{q}_1 + 4\mathbf{P}_1 \cdot \mathbf{P}_2 ], \end{aligned} \quad (21b)$$

$$\begin{aligned} \langle \mathbf{p}'_1, \mathbf{p}'_2, \mathbf{p}'_3 | W_3^{\sigma\omega} | \mathbf{p}_1, \mathbf{p}_2, \mathbf{p}_3 \rangle &= (2\pi)^3 \delta^{(3)}(\mathbf{p}'_3 - \mathbf{p}_3 - \mathbf{q}_1 - \mathbf{q}_2) \frac{g_{\omega N}^2 g_{\sigma N}^2}{4M^3} \\ &\quad \times \left\{ \frac{F_\sigma^2(q_1^2)}{q_1^2 + m_\sigma^2} \frac{F_\omega^2(q_2^2)}{q_2^2 + m_\omega^2} [ -\mathbf{q}_2^2 - i\boldsymbol{\sigma}_3 \cdot ((2\mathbf{p}_3 + \mathbf{q}_1) \times \mathbf{q}_2) \right. \\ &\quad \left. - (2\mathbf{p}_3 + \mathbf{q}_1 + \mathbf{q}_2 + i\boldsymbol{\sigma}_3 \times \mathbf{q}_2) \cdot (2\mathbf{P}_2 - i\boldsymbol{\sigma}_2 \times \mathbf{q}_2) ] + 1 \leftrightarrow 2 \right\}. \end{aligned} \quad (21c)$$

In these expressions we have introduced vertex form factors  $F_{\sigma, \omega}(q^2)$  with the monopole parametrization of Eq. (5). In the Hartree approximation, the only contribution which survives and gives the strong saturation effect is the first term in Eq. (21a) proportional to  $\mathbf{p}_3^2$  (this contribution is not present in the three- and four-body calcula-

tions of Ref. 22). We emphasize here that the 3BF we derive in this section is of the same order as the spin-orbit part of the  $NN$  potential. Moreover, since the meson propagators are treated in the static approximation, there is no ambiguity as far as consistency with the nonrelativistic nuclear wave function is concerned.



#### IV. EVALUATION OF CORRECTIONS AT FINITE NUCLEAR DENSITY

The 3BF of Eqs. (21) supplemented with the  $\pi$ - and  $\rho$ -exchange contributions of Refs. 17 and 18 with parameters determined in Sec. II are used in this section to determine the three-body potential contributions to the binding energy of nuclear matter. We use the formalism of McKellar and Rajaraman<sup>26</sup> which we shortly recall.

##### A. Formalism

The contributions of the 3BF  $W$  to the nuclear binding energy is given by

$$E_W = \sum_{i < j < k} \sum_P \pi_P \langle \Psi_{ijk} | W | \Omega_{P(ijk)} \rangle, \quad (22)$$

where  $|\Psi_{ijk}\rangle$  is the wave function for three particles in the state  $(ijk)$  calculated with the two-body force only, and  $|\Omega_{P(ijk)}\rangle$  is the three-body wave function obtained from both the two-body force and the 3BF  $W$ . The sub-

$$E_W^{(1)} = \frac{1}{2} \sum_{ij} \langle \varphi_i(1) \varphi_j(2) | \left[ 1 - G^{(2)} \frac{Q}{e} \right] V_3 \left[ 1 - \frac{Q}{e} G^{(2)} \right] | \varphi_i(1) \varphi_j(2) - \varphi_j(1) \varphi_i(2) \rangle, \quad (24)$$

where  $\varphi_i(1)$  is a normalized plane wave. The energy contribution per particle due to  $E_W^{(1)}$  is symbolically rewritten as

$$\frac{E_W^{(1)}}{A} = \langle V_3 \rangle - 2 \langle G^{(2)} \frac{Q}{e} V_3 \rangle + \langle G^{(2)} \frac{Q}{e} V_3 \frac{Q}{e} G^{(2)} \rangle. \quad (25)$$

Following the approximations made in Ref. 26, one may reduce  $E_W^{(2)}/A$  to

$$\frac{E_W^{(2)}}{A} = - \langle V_3 \frac{Q}{e} V_3 \rangle. \quad (26)$$

We shall evaluate the effect of  $V_3$  by performing a proper Brueckner calculation with the effective potential  $V_3$  added to the two-body force  $V_2$ . If one denotes by  $G^{(2+3)}$  the reaction matrix built in this way, the energy contribution due to  $W$  will be obtained as

$$\frac{E_W}{A} = \langle \varphi | \Delta G | \varphi \rangle = \langle \varphi | G^{(2+3)} - G^{(2)} | \varphi \rangle. \quad (27)$$

$$V_3(\mathbf{r}'_1, \mathbf{r}'_2 | \mathbf{r}_1, \mathbf{r}_2) = \frac{1}{4} \text{Tr} \sum_n \int d^3 r_3 d^3 r'_3 \varphi_n^*(\mathbf{r}'_3) (1 - \eta(\mathbf{r}'_{13})) (1 - \eta(\mathbf{r}'_{23})) \\ \times W_3(\mathbf{r}'_1, \mathbf{r}'_2, \mathbf{r}'_3 | \mathbf{r}_1, \mathbf{r}_2, \mathbf{r}_3) (1 - \eta(\mathbf{r}_{13})) (1 - \eta(\mathbf{r}_{23})) \varphi_n(\mathbf{r}_3), \quad (29)$$

where the trace is taken with respect to the spin and isospin of nucleon 3 (cf. Fig. 8). To obtain Eq. (29) we have used the solution of the Bethe-Faddeev equation<sup>37</sup> valid for a strongly repulsive central two-body potential. Thereby, we consider only the most important central correlations  $\eta(\mathbf{r}_{13})$  and  $\eta(\mathbf{r}_{23})$  between nucleons (1,3) and

script  $P$  stands for the permutations of  $(ijk)$  with  $\pi_P$  their parities. To our knowledge the complete evaluation of Eq. (22) has only been performed<sup>35</sup> for the bound state three-body problem with the  $2\pi$  exchange 3BF of Ref. 17. A similar evaluation<sup>36</sup> is currently under way with the complete 3BF used here.

To second order in  $W$  one may write

$$E_W = E_W^{(1)} + E_W^{(2)} \\ = \sum_{i < j < k} \sum_P \pi_P \langle \Psi_{ijk} | W - W \frac{Q}{e} W | \Psi_{P(ijk)} \rangle. \quad (23)$$

The neglect of the double exchange term in this expression allows us to define an effective force  $V_3$  which renders the calculation of  $E_W^{(2)}$  tractable. If one specifies the correlation in particles 1 and 2 in the three-body correlated wave function  $|\Psi_{ijk}\rangle$  by those built in by the operator  $1 - G^{(2)} Q/e$ , with  $G^{(2)}$  the Brueckner reaction matrix obtained from the two-body potential  $V_2$  alone, then  $E_W^{(1)}$  takes the form

Using the integral equation obeyed by  $G$ , one readily obtains

$$\langle \varphi | \Delta G | \varphi \rangle = \langle V_3 \rangle - \langle G^{(2)} \frac{Q}{e} V_3 \rangle - \langle V_3 \frac{Q}{e} G^{(2+3)} \rangle \\ + \langle G^{(2)} \frac{Q}{e} V_3 \frac{Q}{e} G^{(2+3)} \rangle, \quad (28)$$

which reduces to the sum of the contributions (25) and (26) when  $G^{(2+3)} \approx G^{(2)} + V_3$ . This procedure of evaluating  $E_w/A$  has been checked and used in the past.<sup>17,20</sup> Although it involves many successive approximations and does not consider certain type of contributions,<sup>17</sup> it offers the interesting possibility of generating directly the important single and exchange contribution present in Eqs. (25) and (26) while the double exchange contribution correcting  $\langle V_3 \rangle$  may be evaluated simply.<sup>20</sup> We show below that the expected saturating features of the 3BF of Sec. III are present in  $\langle V_3 \rangle$ .

Explicitly, the effective force  $V_3$  is given by

(2,3), respectively. Here  $\eta(r)$  is the average over spin and momenta in the Fermi sea of the  $^1S_0$  and  $^3S_1$  partial wave components of the wave defect

$$\eta_{jl}(\mathbf{r}_1, \mathbf{r}_2) = \langle (\mathbf{r}_1, \mathbf{r}_2) | \frac{Q}{e} G_{12} | \mathbf{j}, l \rangle. \quad (30)$$

Generalizing Eq. (29) to include tensor correlations would involve products of terms where  $1-\eta(r)$  are changed to  $1-\eta(r)-S_{ij}(\mathbf{r})\eta^T(r)$ , with  $S_{ij}(\mathbf{r})$  the usual tensor operator and  $\eta^T(r)$  an average wave defect in the channels coupled by the tensor operator, principally  ${}^3S_1+{}^3D_1$ . While  $1-\eta(r)$  reaches unity<sup>25</sup> for  $r \geq 0.8-1$  fm,  $\eta^T(r)$  remains small ( $<0.2$ ) for all  $r$  thereby effectively reducing contributions with factors of  $\eta^T(r)$  in the integrand of Eq. (29) with respect to those with factors of  $1-\eta(r)$  only. A full scale Bethe-Faddeev calcula-

tion with  $W$  is probably the only way to do better.

To obtain  $W_3(\mathbf{r}'_1, \mathbf{r}'_2, \mathbf{r}'_3; \mathbf{r}_1, \mathbf{r}_2, \mathbf{r}_3)$  we take the Fourier transforms of the expressions (21) [multiplied by  $(2\pi)^{-9}$  for correct normalization] with respect to the variables  $(\mathbf{p}'_1, \mathbf{p}'_2, \mathbf{p}'_3; \mathbf{p}_1, \mathbf{p}_2, \mathbf{p}_3)$ . We give here the full result for the  $2\sigma$ -exchange 3BF as we shall use it in the later discussion. The other contributions from  $\sigma\omega$  and  $2\omega$  exchanges are given in Appendix A. We write  $\mathbf{x}=\mathbf{r}'_3-\mathbf{r}_1$ ,  $\hat{\mathbf{x}}=\mathbf{x}/|\mathbf{x}|$ , and  $\mathbf{y}=\mathbf{r}'_3-\mathbf{r}_2$ . The  $2\sigma$ -exchange 3BF is nonlocal in the variables  $(\mathbf{r}'_3, \mathbf{r}_3)$  and writes

$$\begin{aligned}
 W_3^{2\sigma}(\mathbf{x}, \mathbf{y}; \mathbf{r}'_3 | \mathbf{r}_3) = & \frac{g_{\sigma N}^4}{4M^3} \frac{m_\sigma^2}{(4\pi)^2} \delta^{(3)}(\mathbf{r}'_1 - \mathbf{r}_1) \delta^{(3)}(\mathbf{r}'_2 - \mathbf{r}_2) \\
 & \times \left\{ -4Z_\sigma(\mathbf{x})Z_\sigma(\mathbf{y})\nabla_{r'_3}^2 - 4Z'_\sigma(\mathbf{x})Z_\sigma(\mathbf{y})\hat{\mathbf{x}} \cdot \nabla_{r'_3} - 4Z_\sigma(\mathbf{x})Z'_\sigma(\mathbf{y})\hat{\mathbf{y}} \cdot \nabla_{r'_3} \right. \\
 & - \left[ \left[ Z''_\sigma(\mathbf{x}) + \frac{2}{x}Z'_\sigma(\mathbf{x}) \right] Z_\sigma(\mathbf{y}) + Z_\sigma(\mathbf{x}) \left[ Z''_\sigma(\mathbf{y}) + \frac{2}{y}Z'_\sigma(\mathbf{y}) \right] \right] - \hat{\mathbf{x}} \cdot \hat{\mathbf{y}} Z'_\sigma(\mathbf{x})Z'_\sigma(\mathbf{y}) \\
 & \left. - 2i[Z'_\sigma(\mathbf{x})Z_\sigma(\mathbf{y})\sigma_3 \cdot (\hat{\mathbf{x}} \times \nabla_{r'_3}) + Z_\sigma(\mathbf{x})Z'_\sigma(\mathbf{y})\sigma_3 \cdot (\hat{\mathbf{y}} \times \nabla_{r'_3})] \right\} \delta^{(3)}(\mathbf{r}'_3 - \mathbf{r}_3). \quad (31)
 \end{aligned}$$

Here the function  $Z_\sigma(\mathbf{x})$  is given by

$$Z_\sigma(\mathbf{x}) = \frac{4\pi}{m_\sigma} \int \frac{d^3q}{(2\pi)^3} \frac{e^{i\mathbf{q} \cdot \mathbf{x}} F_\sigma^2(q^2)}{(q^2 + m_\sigma^2)}. \quad (32)$$

With the form factor  $F_\sigma(q^2)$  defined in Eq. (5),  $Z_\sigma(\mathbf{x})$  and its single and double derivatives  $Z'_\sigma(\mathbf{x})$  and  $Z''_\sigma(\mathbf{x})$  are obtained in a closed form.<sup>18</sup> Had we kept in Eq. (21a) only the terms involving the momentum transfer  $(\mathbf{q}_1, \mathbf{q}_2)$  we would have obtained the fourth and fifth terms in Eq. (31) and only this one when no form factors are considered and contact terms are disregarded as in Ref. 22.

In the derivation of the effective force  $V_3$  from Eq. (29) let us focus on the first term in Eq. (31) and denote this contribution by  $V_3^{2\sigma,1}$ , local in the variables  $(\mathbf{r}_1, \mathbf{r}_2)$ . With  $g(\mathbf{x})=1-\eta(\mathbf{x})$ , it writes

$$\begin{aligned}
 V_3^{2\sigma,1}(r_{12}) = & -\frac{g_{\sigma N}^4}{4M^3} \frac{m_\sigma^2}{(4\pi)^2} \frac{1}{\Omega} \sum_{\substack{m_{s_3}, m_{r_3} \\ \hat{\mathbf{p}}_n}} \theta(k_F - |\mathbf{p}_n|) \int d^3r_3 \left[ \int d^3r'_3 e^{i\mathbf{p}_n \cdot \mathbf{r}'_3} g(|\mathbf{r}'_3 - \mathbf{r}_1|) g(|\mathbf{r}'_3 - \mathbf{r}_2|) \right. \\
 & \left. \times Z_\sigma(|\mathbf{r}'_3 - \mathbf{r}_1|) Z_\sigma(|\mathbf{r}'_3 - \mathbf{r}_2|) \nabla_{r'_3}^2 \delta^{(3)}(\mathbf{r}'_3 - \mathbf{r}_3) \right] \\
 & \times g(|\mathbf{r}_3 - \mathbf{r}_1|) g(|\mathbf{r}_3 - \mathbf{r}_2|) e^{-i\mathbf{p}_n \cdot \mathbf{r}_3}, \quad (33a)
 \end{aligned}$$

$$\begin{aligned}
 = & \frac{g_{\sigma N}^4}{M^3} \frac{m_\sigma^2}{(4\pi)^2} \left\{ \frac{3}{5} \left[ \frac{3\pi^2}{2} \right]^{2/3} \rho_B^{5/3} \int d^3r_3 g^2(\mathbf{x}) g^2(\mathbf{y}) Z_\sigma(\mathbf{x}) Z_\sigma(\mathbf{y}) \right. \\
 & - \rho_B \int d^3r_3 g(\mathbf{x}) g(\mathbf{y}) \left[ \left[ g''(\mathbf{x}) + \frac{2}{x}g'(\mathbf{x}) \right] g(\mathbf{y}) + g(\mathbf{x}) \left[ g''(\mathbf{y}) + \frac{2}{y}g'(\mathbf{y}) \right] \right. \\
 & \left. \left. + 2\hat{\mathbf{x}} \cdot \hat{\mathbf{y}} g'(\mathbf{x}) g'(\mathbf{y}) \right] Z_\sigma(\mathbf{x}) Z_\sigma(\mathbf{y}) \right\}. \quad (33b)
 \end{aligned}$$

Here  $\hat{\mathbf{x}} \cdot \hat{\mathbf{y}} = (x^2 + y^2 - r^2)/(2xy)$  and  $\int d^3r_3 = 2\pi/r \int_0^\infty x dx \int_{|r-x|}^{r+x} y dy$ .

In the absence of nucleon-nucleon correlations, as was the case in the development of Sec. III A,  $g(\mathbf{x})=1$ , the second term in Eq. (33b) drops out and the Hartree contribution to  $\langle V_3 \rangle$  in Eq. (25) reduces to

$$\begin{aligned}
 \langle V_3^{2\sigma,1} \rangle_H = & \frac{\rho_B}{2} \int d^3r V_3^{2\sigma,1}(r) \\
 = & \frac{1}{2} \frac{3}{5} \left[ \frac{3\pi^2}{2} \right]^{2/3} \frac{g_{\sigma N}^4}{M^3 m_\sigma^4} \rho_B^{8/3} \left[ 1 - \frac{m_\sigma^2}{\Lambda_\sigma^2} \right]^4. \quad (34)
 \end{aligned}$$

TABLE II. Various contributions (in MeV) to the potential energy at three typical baryonic densities.

Density	(S, T)	$V_2$	$V_2 + V_3(\pi, \rho)$	$V_2 + V_3(\pi, \rho) + V_3(\sigma, \omega - \bar{N})$	$V_2 + V_3(\pi, \rho) + V_3(\sigma, \omega - \bar{N}, R)$
$\rho_0/2$	(1,0) <sup>a</sup>	-27.18	-26.36	-25.69	-26.38
	(0,1) <sup>a</sup>	-21.53	-19.67	-19.14	-19.71
	(1,1) <sup>b</sup>	-0.14	-1.14	-0.84	-1.74
	(0,0) <sup>b</sup>	5.01	3.96	4.02	3.91
	$U$	-43.84	-43.21	-41.65	-43.92
	$E/A$	-6.85	-6.55	-5.76	-6.90
$\rho_0$	(1,0) <sup>a</sup>	-44.70	-41.47	-39.52	-40.53
	(0,1) <sup>a</sup>	-37.17	-30.35	-28.34	-30.09
	(1,1) <sup>b</sup>	0.16	-5.82	-3.88	-7.86
	(0,0) <sup>b</sup>	10.99	5.95	6.27	5.87
	$U$	-70.72	-71.69	-65.47	-72.61
	$E/A$	-12.33	-12.82	-9.71	-13.28
$2\rho_0$	(1,0) <sup>a</sup>	-78.30	-47.39	-34.04	-42.07
	(0,1) <sup>a</sup>	-65.14	-35.83	-24.85	-32.27
	(1,1) <sup>b</sup>	4.00	-18.69	-3.94	-22.64
	(0,0) <sup>b</sup>	24.44	4.18	6.38	4.31
	$U$	-115.00	-97.73	-56.45	-92.67
	$E/A$	-21.52	-12.88	-7.75	-10.36

<sup>a</sup>Summation on partial waves with  $l \leq 4$ .

<sup>b</sup>Idem but with  $l \leq 5$ .

With the values of Table I for the coupling constants, regulator masses and a scalar meson mass  $m_\sigma = 540$  MeV, we obtain

$$\langle V_3^{2\sigma,1} \rangle_H = 3.9 \text{ MeV} \left( \frac{\rho_B}{\rho_0} \right)^{8/3}, \quad (35)$$

close to the result of Eq. (17). This is quite remarkable considering that the consistency requirements discussed in Sec. III invoke physical considerations other than the simple empirical fixing of parameters on nuclear saturation properties as in the " $\sigma$ - $\omega$ " model.

It is clear now that the dominating saturating features of the  $2\sigma$ -exchange term resides in the individual momentum dependence of the nucleons.<sup>12</sup> Hence keeping only terms involving transferred momenta<sup>22</sup> misses an essential piece of the  $2\sigma$ -exchange 3BF. In the nuclear medium at finite density the net saturating effect of using the full  $V_3^{2\sigma}(r_{12})$  is expected to be somewhat reduced with respect to the result of Eq. (35). It is due, on the one hand, to the presence of correlations [ $g(x) \neq 1$ ] and of the exchange Fock term in  $\langle V_3 \rangle$ , and, on the other hand, to the other contributions ( $\sigma\omega$  and  $2\omega$  of Fig. 8) to the effective force  $V_3$  which come in with different signs. Because of their length these contributions are given in Appendix A. However, as the nuclear density increases the term in  $\rho_B^{5/3}$  in Eq. (33b) will gradually take over all the other terms linear in  $\rho_B$  thereby stiffening the equation of state with respect to the one involving the Paris potential alone or eventually supplemented with conventional  $2\pi$ -,  $\pi\rho$ -, and  $2\rho$ -exchange 3BF.<sup>17</sup>

### B. Numerical results

The results of nuclear matter binding energy calculations as a function of density for the Paris potential<sup>23</sup>

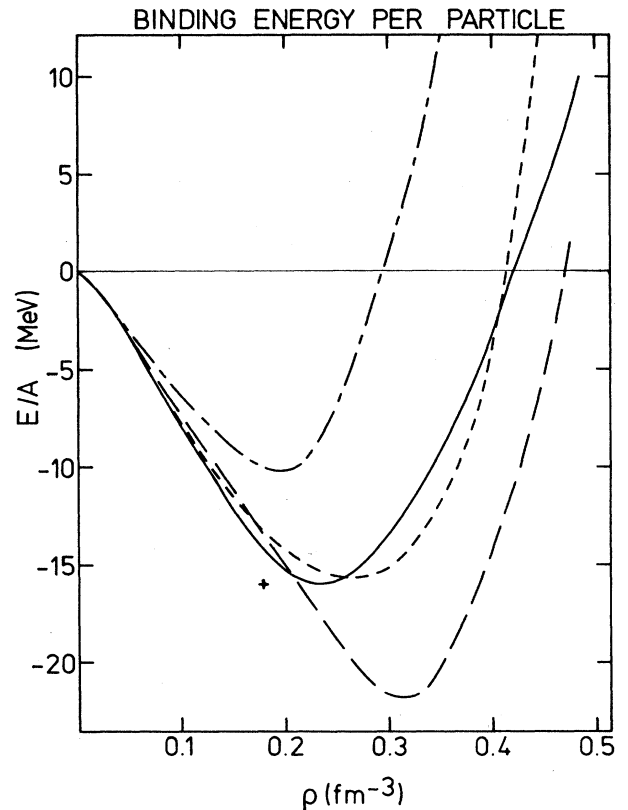


FIG. 9. Binding energy per particle as function of symmetric nuclear matter density: long-dashed line: Paris potential only; short-dashed line: Paris potential and  $(\pi, \rho)$  effective two-body force; dash-dotted line: Paris potential,  $(\pi, \rho)$  and  $(\sigma, \omega) - \bar{N}$  effective two-body forces; continuous line: Paris potential,  $(\pi, \rho)$ ,  $(\sigma, \omega) - \bar{N}$ , and  $(\sigma, \omega) - R$  effective two-body forces. The cross in this figure indicates the empirical saturation point.

alone are well established.<sup>4,25,34</sup> Here we adopt the calculation scheme of Ref. 25 based upon the continuous choice of Jeukenne *et al.*<sup>38</sup> for the auxiliary single particle field. This approach is essentially a modified version of the Brueckner-Bethe (BHF) hole line expansion<sup>4</sup> and its motivations and validity in comparison with alternative techniques have been extensively discussed in the past.<sup>38,39</sup> In Table II, we indicate under the column  $V_2$  and for the three densities  $\rho_0/2, \rho_0$  and  $2\rho_0$ , respectively, with  $\rho_0 = 0.17 \text{ fm}^{-3}$  the density at empirical saturation, the different contributions in each spin and isospin subspace to the nuclear matter potential energy per particle for the Paris potential. The corresponding saturation curve is shown in Fig. 9 by the long dashed line. It is the modifications with respect to this situation and brought about by the effective force  $V_3$  we want to investigate. Although we are confident to identify the correct saturation trends, as argued in Sec. III A, we stress that the only way in our framework to be more precise is to solve the Bethe-Faddeev equation in the presence of the 3BF  $W$ .

We investigate first the effects of the 3BF  $V_3$  due to  $2\pi$ -,  $\pi\rho$ -, and  $2\rho$ -exchanges only, as given by Eqs. (4.7), (4.9), and (4.10) of Ref. 17 for the  $2\pi$  part and by Eqs. (3.10) to (3.13) of Ref. 18, for the  $\pi\rho$ -, and  $2\rho$  parts. [Eq. (4.10c) of Ref. 17 has to be corrected for a misprint:  $2\eta^4/\mu^2$  has to be replaced by  $2\eta^6/\mu^4$ . Same remark for Eq. (3.13) of Ref. 18 where  $\frac{1}{3}$  in the first factor has to be replaced by 3.] The coupling constants, masses and regulator masses are those of Table I. Here and in all the cases discussed below, we perform a fully self-consistent calculation of the reaction matrix  $G^{(2+3)}$ .

The effective potential  $V_3^{(\pi,\rho)}$  can be separated into central and tensor components  $V_{3,C}^{(\pi,\rho)}$  and  $V_{3,T}^{(\pi,\rho)}$

$$V_3^{(\pi,\rho)}(\mathbf{r}) = \tau_1 \cdot \tau_2 (\sigma_1 \cdot \sigma_2 V_{3,C}^{(\pi,\rho)}(r) + S_{12}(\hat{\mathbf{r}}) V_{3,T}^{(\pi,\rho)}(r)). \quad (36)$$

Each component is the sum of  $2\pi$ -,  $\pi\rho$ -, and  $2\rho$ -contributions. In symmetric nuclear matter, the tensor part contributes only through terms in  $Q/e$  in Eq. (28) and corrections to the first order perturbative results  $\langle V_3 \rangle$  may be expected depending upon the intensity of  $V_3$ . Detailed accounts on this aspect of the problem are given in Refs. 17 and 19. The results are given in Table II, under the column  $V_2 + V_3^{(\pi,\rho)}$ . The different contributions in each  $(S, T)$  subspace reflect the spin-isospin structure in Eq. (36) and the overall attractive character of  $V_{3,C}^{(\pi,\rho)}$ . The corresponding saturation curve is shown in Fig. 9 by the short dashed line. These results have to be compared with those of Ref. 25 where a less sophisticated 3BF was used with no attention paid to the consistency requirements of Sec. II. As already noted in Ref. 17, the additional attraction we obtain at low density with respect to results of Ref. 25 originates from components in the  $2\pi$ -3BF not present in the 3BF version used there.

In Table II we compare the complete estimate of  $E_w/A$  from Eq. (27) to the first term  $\langle V_3 \rangle$  of Eq. (28). For the purpose of comparison and because of the changes in parameters with respect to earlier studies (cf. Sec. II and Table I) we show in Fig. 10 at normal nuclear density, the different contributions building up the total

$V_{3,C}^{(\pi,\rho)}$  and  $V_{3,T}^{(\pi,\rho)}$  in MeV as a function of the distance  $r$  in fm. They noticeably differ from those of Ref. 18 not only due to changes in parameters but more importantly because of the very different correlation function  $\eta(r)$  induced<sup>25</sup> by the Paris potential as compared to the one induced by the Reid soft core interaction.

We turn now to the study of the corrections from the effective force  $V_3$  due to  $2\sigma$ -,  $2\sigma\omega$ -, and  $2\omega$ -exchanges derived from Sec. III B with the values of coupling constants, masses and regular masses obtained in Sec. II and gathered in Table I. From the constraints discussed in that section we obtain at zero density a  $\sigma$ -meson mass of about 680 MeV. We recall that it is expected to decrease substantially with increasing nuclear density because of medium corrections.<sup>29,30</sup> The actual  $m_\sigma$  arrived at and used in relativistic mean field calculations is around 500–550 MeV. We choose here to work with a constant  $\sigma$ -meson mass of 540 MeV which is actually the value read off from Fig. 2 of Ref. 30 at normal density. We shall present and discuss at the end of the next section the overall effect on the saturation curve one may expect when considering medium corrections to the  $\sigma$  mass.

To the contributions  $V_3^{(\pi,\rho)}$  we add now those of Eq. (33) and Eqs. (A4) to (A9) of Appendix A and perform a new self-consistent calculation of the reaction matrix  $G^{(2+3)}$ . The results are again given in Table II, where under the columns  $V_2 + V_3^{(\pi,\rho)} + V_3^{(\sigma,\omega-\bar{N})}$ , appear the different subspace contributions to the nuclear matter po-

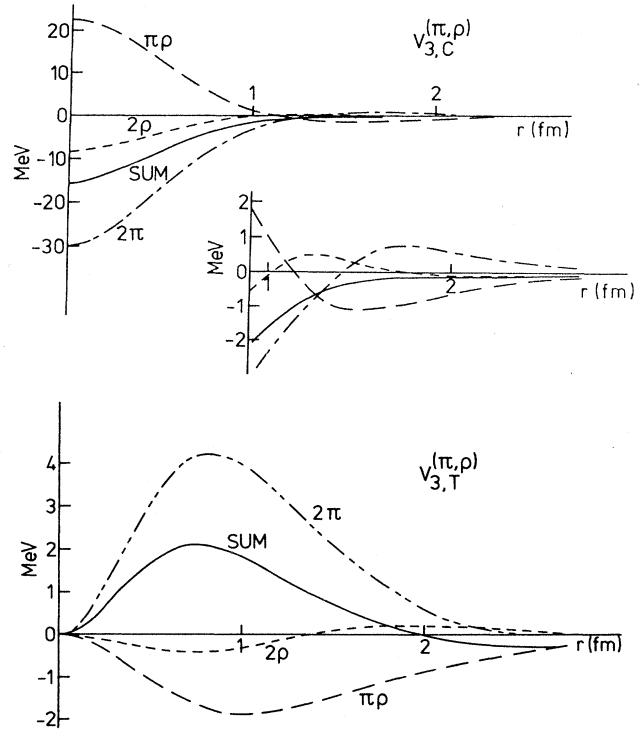


FIG. 10. (a) The  $2\pi$ -,  $\pi\rho$ -, and  $2\rho$ -contributions to the spin-spin two-body effective force  $V_{3,C}^{(\pi,\rho)}$  of Eq. (36) at baryonic density  $\rho_B = 0.17 \text{ fm}^{-3}$ ; (b) same as (a) for the tensor two-body effective force.

TABLE III. Various contributions to  $\Delta G$  and  $V_3$  [see Eqs. (27) and (28)], from the different pieces of the three-body force.

Density	$(\pi, \rho)-\Delta$	$2\sigma-\bar{N}(\rho_B^{8/3})$	$2\sigma-\bar{N}(\rho_B^2)$	$2\omega-\bar{N}$	$\sigma\omega-\bar{N}$	Sum	$(\sigma, \omega)-R$
$\rho_0/2$ $\langle \Delta G \rangle$	0.30	0.23	-0.17	-0.07	0.76	1.05	-1.02
						(1.09)	(-1.14)
$\rho_0$ $\langle \Delta G \rangle$	-0.49	1.43	-0.80	-0.26	3.16	3.04	-4.24
						(2.62)	(-3.57)
$2\rho_0$ $\langle \Delta G \rangle$	8.64	10.03	-3.43	-1.12	14.56	28.68	-18.13
						(29.27)	(-18.11)
$\langle V_3 \rangle$		1.20	-0.79	-0.25	2.65	2.81	-4.21
		9.10	-3.55	-1.21	13.26	17.60	-18.44

tential energy per particle. The corresponding saturation curve is shown in Fig. 9 by the dash-dotted line. In Table III we have separated the contribution to the energy in  $\rho_B^{8/3}$  coming from the first term in Eq. (33) from those in  $\rho_B^2$ . The results were obtained from a calculation (cf. Sec. IV A) of  $G^{(2)}$  and of  $G^{(2+3)}$  with an effective two-body potential corresponding only to the component under consideration, that is the first term of Eq. (33) for the case  $2\sigma-\bar{N}(\rho_B^{8/3})$ , the second term of Eq. (33) and the contribution of Eq. (A4) for  $2\sigma-\bar{N}(\rho_B^2)$ , contributions from Eqs. (A5) to (A8) for  $2\omega-\bar{N}$ , and the contribution from Eq. (A9) for  $\sigma\omega-\bar{N}$ . The single particle spectra used at each density in the evaluation of both  $G^{(2)}$  and  $G^{(2+3)}$  is the self-consistent one corresponding to the calculation at the same density of the third column of Table II. Under the column "sum" figures the sum of the different contributions to  $\langle \Delta G \rangle$ . The numbers in parentheses are those obtained from Table II ( $\Delta E/A$  from columns 3 and 1 in that table) and differ slightly from the sum in Table III because of the different single particle spectra used in evaluating  $G^{(2)}$ .

The effective potential  $V_3$  is only central for  $2\sigma$  and  $\sigma\omega$  contributions but receives central, spin-spin, and tensor components from  $2\omega$  contributions (cf. Appendix A). The different components in MeV are shown in Fig. 11 as a function of  $r$  in fm. The central component is altogether dominant and the  $2\omega$  tensor component is seen to be much smaller than its  $(\pi, \rho)$  counterpart, hence bringing  $\langle \Delta G \rangle$  much closer to  $\langle V_3 \rangle$  than in the  $(\pi, \rho)$  case. It is plain to see that for the most dominant  $\sigma$  and  $\omega$  contributions, the predominance of  $\langle V_3 \rangle$  occurs thereby comforting our approximate treatment of the 3BF  $W$  made in Sec. IV A. We do not expect, as we argued, that the tensor correlations left out in the evaluation of the effective force from Eq. (29) and double exchange contributions would invalidate this result and jeopardize the saturation mechanism brought about by  $V_3$ .

Going back to Table III, it is of interest to compare the value of the Hartree contribution obtained in Sec. IV [Eq. (35)] with the value of  $\langle V_3 \rangle$  in  $\rho_B^{8/3}$ . The latter includes the effect of correlations and the exchange-Fock contribution. We obtain, respectively,

$$\begin{aligned}
 \rho = \rho_0/2: \langle V_3^{2\sigma,1} \rangle_{H,Cor} &= 0.3 \text{ MeV}, \quad \langle V_3^{2\sigma,1} \rangle_{F,Cor} = -0.1 \text{ MeV}, \\
 \rho = \rho_0: \langle V_3^{2\sigma,1} \rangle_{H,Cor} &= 1.6 \text{ MeV}, \quad \langle V_3^{2\sigma,1} \rangle_{F,Cor} = -0.4 \text{ MeV}, \\
 \rho = 2\rho_0: \langle V_3^{2\sigma,1} \rangle_{H,Cor} &= 11.4 \text{ MeV}, \quad \langle V_3^{2\sigma,1} \rangle_{F,Cor} = -2.3 \text{ MeV}.
 \end{aligned} \tag{37}$$

For the Hartree term a slight departure from the  $\rho_B^{8/3}$  law occurs due to the density dependence of the correlation function  $\eta(r)$  which, for the Fock term, combines with the usual Fermi momentum dependence of the exchange integral. The effect of the short-range  $NN$  correlations reduces the estimate of Eq. (35) by a factor close to 2.5, in keeping with the results of relativistic Dirac-Brueckner calculations of the reaction matrix.<sup>10,11</sup> Up to a nuclear density of about  $2.5\rho_0$ , the  $(\sigma-\omega)$ -contributions of Fig. 11 linear in  $\rho_B$  overrides the  $2\sigma$  contributions in  $\rho_B^{5/3}$  but the latter is nevertheless instrumental in driving the position of the saturation density to a lower value, at variance with the result of Ref. 21. The huge reduction in binding we observe from the long dashed to the dash-dotted curve of Fig. 9 may actually seem to question our whole approach to corrections to the two-body potential results.

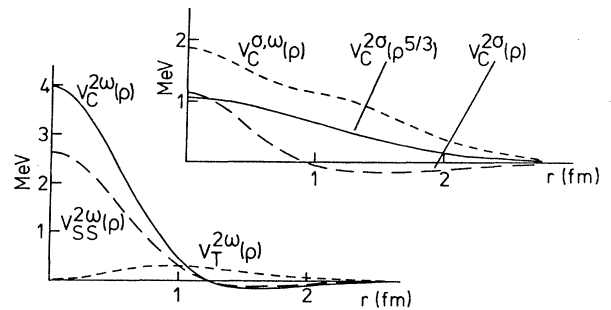


FIG. 11. The  $2\sigma$ -,  $\sigma\omega$ -, and  $2\omega-N$  contribution to the central two-body effective force and the  $2\omega$  contribution to the spin-spin and tensor two-body effective force. The baryonic density is  $\rho_B = 0.17 \text{ fm}^{-3}$ .

However, this is not the case as these corrections have to be confronted with the total potential energy  $U$  in the column  $V_2$  of Table II and are at most of the order of 20% of this quantity.

At this stage, some remarks about the mass of the  $\sigma$  meson are in order. Throughout our calculations we have adopted a value  $m_\sigma = 540$  MeV. This is consistent with the results of Ref. 30 in which the  $\sigma$ -meson is described as a quark-antiquark quasibound state. This model being rather successful in describing pion physics<sup>40</sup> we may tend to consider this value of  $m_\sigma$  as rather compelling. However, it is worth noting that the value arrived at in Ref. 32 is only  $m_\sigma = 440$  MeV, emphasizing the importance of medium effects hidden in this fictitious  $\sigma$ -meson mass. The important point we want to stress here is that whatever the mass  $m_\sigma$  retained in the common range 450 to 600 MeV, the saturation curve including three-body pair term contributions will be driven up from the short-dashed one in Fig. 9 with  $(\pi, \rho)$  three-body forces towards the dash-dotted curve in the same figure. Clearly the question arises about the genuine mechanism possibly leading to additional attraction in agreement with the empirical saturation.

## V. CONTRIBUTION OF EXCITED STATES

### A. Model for the Roper resonance

The second contribution to the 3BF we are interested in is given in Fig. 3(b), second diagram, and is related to the occurrence of nucleon excitations in the intermediate state.<sup>41,42</sup> This is of course a direct and unavoidable consequence of the composite structure of the nucleon, and must be considered on the same footing as the contribution of  $N\bar{N}$  pair terms studied in the preceding section. For  $\sigma$  and  $\omega$  exchange, the only resonances which can be excited are those with  $J = T = \frac{1}{2}$ . The first candidate is the Roper resonance of mass  $M_R = 1440$  MeV, which is strongly coupled to  $\pi N$  and  $\pi\pi N$  channels. The excitation of the Roper resonance through  $\pi$  and  $\rho$  exchange is implicitly included in the derivation of Ref. 17 and already considered in the previous section.

Very little is known about the Roper resonance, both from an experimental and theoretical point of view. For our purpose, the most interesting experimental quantity is its decay width into  $\pi N$

$$\Gamma_{R \rightarrow \pi N}^{\text{exp.}} = \begin{cases} 65 \text{ MeV} \\ 205 \text{ MeV} \end{cases}, \quad (38)$$

where we indicate the two available measurements.<sup>43</sup> From these data, one can extract the  $\pi NR$  coupling constant, provided the form factor at the vertex is known.

Theoretically, the Roper resonance is not yet fully understood. Being a radial excitation of the nucleon, the simplest configuration is a 1particle-1hole quark excitation, i.e., a quark in the  $1s_{1/2}$  is excited in the  $2s_{1/2}$  level. This configuration is commonly assumed in the constituent quark model for the nucleon structure. This however raises the unanswered question of the position of the 1p excitation ( $N^*$  of mass 1535 MeV) at a higher position in energy than the Roper, though its excitation is only  $1h\omega$

instead of  $2h\omega$  for the Roper. Qualitatively, this puzzle may be discussed in several ways. First of all, the Roper resonance may be a collective excitation rather than a simple 1p-1h configuration, and therefore its excitation energy can be lowered. This can be investigated for instance in a RPA type calculation. Yet no firm conclusions have been reached, as the residual interaction is of foremost importance, and its knowledge is rather limited at present. Secondly, the excitation energy of the negative parity state  $N^*$  could be increased if a more realistic model for the nucleon structure is used. In the chiral bag model for instance, pion self-energy as well as gluonic corrections can reconcile to some extent the experimental spectrum.<sup>44</sup> Finally, it is very attractive to represent, in the bag model, the Roper resonance as a breathing mode of the bag surface.<sup>45,46</sup> The whole spectrum would be thus interpreted as rotational and vibrational states. Yet quantitative spectral predictions are not available.

It is certainly not our purpose to discuss in detail the nature of the Roper resonance, but rather to illustrate how it contributes to the 3BF in nuclei. Hence, we consider here a simple 1p-1h configuration which permits the evaluation of such contribution. The quark wave functions for the  $1s_{1/2}$  and  $2s_{1/2}$  levels are calculated in the color-dielectric model for the nucleon.<sup>27,47</sup> We restrict ourself for simplicity to the SU(2) derivation, keeping only the scalar dielectric field  $\chi$ . The effective Lagrangian we start from is

$$a^4 \mathcal{L} = \chi \bar{q} (i \gamma_\mu \partial^\mu - m_q) q + \frac{1}{3} \beta \chi^2 \partial_\mu \chi \partial^\mu \chi - 4 \lambda^2 \chi^2 (1 + \mu \chi^2 - \nu \chi), \quad (39)$$

where  $q$  is the quark field and  $m_q$  the effective quark mass. The Lagrangian is written here in dimensionless units, the length scale being fixed by the lattice spacing  $a$  after block-spin iterations. Note that the effective quark mass in Eq. (39) should not be confused with the current quark mass. It includes in addition contributions from the expectation value of  $\bar{q}q$  (à la Nambu-Jona-Lasinio for instance). The restoration of chiral symmetry in this model can be done in the usual way by coupling the quarks to the chiral fields  $\phi$  and  $\pi$  according to the  $\sigma$ -model coupling

$$\mathcal{L} = -g \bar{q} (\phi + i \gamma_5 \tau \cdot \pi) q. \quad (40)$$

In the Lagrangian, Eq. (39), it is important to note that the kinetic energy term for the dielectric field  $\chi$  is  $\chi^2 \partial_\mu \chi \partial^\mu \chi$ . This comes from the plaquette summation on the lattice after block spinning. Because of this non-linear structure, the  $\chi$  field has no longer the usual Yukawa asymptotic tail, but goes to zero at some distance  $R_C$  which is determined numerically by solving the equations of motion in the mean-field approximation. This solution leads therefore to an *absolute* confinement of the quarks (analogous to the MIT bag model), at variance to the commonly assumed form  $\partial_\mu \chi \partial^\mu \chi$ . We show in Fig. 12 a typical profile for the dielectric field in the classical limit, normalized to unity, as well as the upper and lower components of the quark wave function  $\varphi$ , in the  $1s_{1/2}$  level, written as

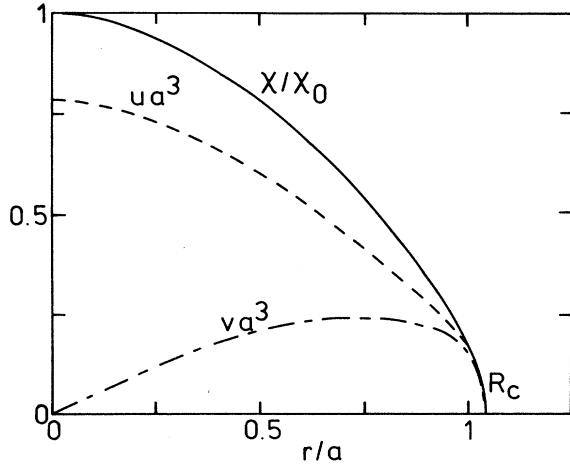


FIG. 12. Color dielectric field  $\chi$  (normalized to unity at  $r=0$ ), and the upper and lower components of the quark wave function in the nucleon, in dimensionless units.

$$\varphi(r) = \frac{1}{\sqrt{\pi}} \begin{pmatrix} u(r) \\ v(r)\sigma \cdot \hat{\mathbf{r}} \end{pmatrix} \frac{1}{\sqrt{\chi(r)}}, \quad (41)$$

for  $r < R_c$ . The normalization is  $\int_0^{R_c} (u^2 + v^2) r^2 dr = 1$ . The parameters in Eq. (39) are fixed to the values  $\mu=0.75$ ,  $\beta=10$ ,  $\lambda^2=5$ ,  $\nu=1.67$ , and  $m_q a = 0.1$ . In order to calculate the various coupling constants and form factors, we couple the external fields  $\sigma$ ,  $\omega$ , and  $\pi$  to the individual quarks in a way similar to Eq. (40). One can thus deduce the following strengths

$$\begin{aligned} g_{\sigma NR}(k) &= 3g_{\sigma q} \int_0^\infty dr j_0(kr) (u_{1s} u_{2s} - v_{1s} v_{2s}) dr \\ g_{\omega NR}(k) &= 3g_{\omega q} \int_0^\infty dr j_0(kr) (u_{1s} u_{2s} - v_{1s} v_{2s}) dr \\ \frac{f_{\pi NR}(k)}{m_\pi} &= -\frac{5}{3} g_{\pi q} \int_0^\infty r dr j_1(kr) (u_{1s} v_{2s} + v_{1s} u_{2s}) dr, \end{aligned} \quad (42)$$

where we denote by  $u_{1s}, v_{1s}$  and  $u_{2s}, v_{2s}$  the 1s and 2s quark wave functions, respectively.

With such form factors and coupling constants, the decay width of the Roper into  $\pi N$  can be written as<sup>45</sup>

$$\Gamma_{R \rightarrow \pi N} = \frac{f_{\pi NR}^2(\bar{k})}{4\pi} \frac{6\bar{k}^3}{m_\pi^2} \frac{M_R - \omega_\pi(\bar{k})}{M_R}, \quad (43)$$

where  $\bar{k}$  is the momentum of the emitted pion, close to 420 MeV/c, and  $\omega_\pi(\bar{k})$  the pion energy.

In order to determine completely the various form factors and coupling constants, one needs to fix the meson-quark coupling strengths and the length scale  $a$ . This is done by calculating the meson-nucleon coupling constants in this model, and thus the meson-quark coupling constants are fixed to get the values reported in Table I and extracted from the Paris potential, following our discussion in Sec. II. The length scale  $a$  is fixed to get the  $\pi NN$  cutoff parameter  $\Lambda$  reported in this table.

With these assumptions, the  $\sigma NN$  cutoff parameter is equal to 1.55 GeV/c, while the cutoff for the  $\omega NN$  and  $\pi NN$  vertices are given in Table I. The difference be-

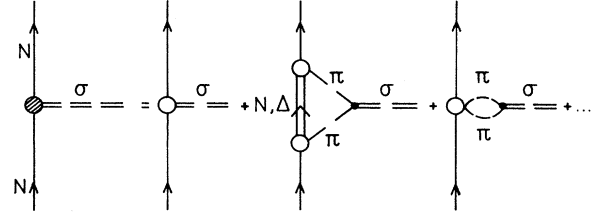


FIG. 13. Various contributions to the  $\sigma NN$  form factor. The first diagram on the right-hand side represents the direct coupling of the  $\sigma$  meson to the quark, while the other contributions involve corrections associated with the coupling to  $2\pi$ .

tween this value and the cutoff of 1.1 GeV/c reported in Table I is attributed to additional vertex renormalization at the  $\sigma NN$  vertex from the coupling of the  $\sigma$  to  $2\pi$ . We indicate schematically in Fig. 13 the various contributions to the  $\sigma NN$  vertex. In the case of the  $\omega NN$  and  $\pi NN$  vertices, such additional renormalization involve at least  $\pi$  and  $\rho$  exchange and are far less important. We have neglected them here.

One can thus calculate all the required coupling constants and form factors for the meson-nucleon-Roper (MNR) vertex. The vertex factors given in Eq. (42) are parametrized as follows

$$\begin{aligned} g_{MNR}(k^2) &= g_{MNR} \frac{\Lambda^2 + \alpha k^2}{\Lambda^2 - \alpha m^2} \left[ \frac{\Lambda^2 - m^2}{\Lambda^2 + k^2} \right] \\ &\equiv g_{MNR} F_M^R(k^2), \end{aligned} \quad (44)$$

and the values for  $\Lambda$ ,  $\alpha$ , and  $g_{MNR}$  are reported in Table I. The  $\sigma NR$  cutoff parameter has been corrected by the same factor as the  $\sigma NN$  vertex (from Fig. 13).

With these parameters, the decay width of the Roper resonance into  $\pi N$  is

$$\Gamma_{R \rightarrow \pi N}^{\text{The.}} \approx 70 \text{ MeV}. \quad (45)$$

This is consistent with the experimental data mentioned in Eq. (38). These parameters can thus be used with some confidence to calculate the contribution to the Roper resonance to the 3BF in nuclear matter.

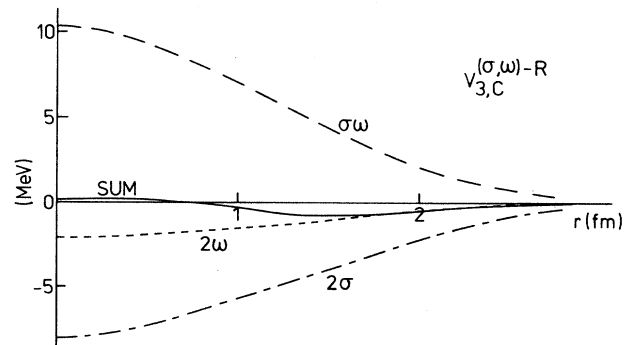


FIG. 14. The  $2\sigma$ ,  $\sigma\omega$ , and  $2\omega$ -R contributions to the central two-body effective force at baryonic density  $\rho_B = 0.17 \text{ fm}^{-3}$ . The continuous curve represents the sum of these three contributions.

### B. Numerical results

The contribution of the 3BF indicated in Fig. 3(b), second diagram is evaluated following the procedure detailed in Sec. III B. The three-nucleon potential  $W$  defined in Eq. (18) is explicit in momentum space in Appendix B, together with the corresponding effective two-body potential  $V_3$ . Note that the potential  $W$  is calculated up to terms in  $q^2/M^2$ , to be consistent with the derivation of the 3BF involving  $N\bar{N}$  excitations. These corrections are far from being negligible. At that order, the meson propagators are also treated in the static approximation.

The contribution to the potential energy are summarized in Tables II and III, and the effective two-body potential shown in Fig. 14. The total potential results from a large cancellation between the  $2\sigma$  and  $2\omega$  part on the one hand, and the  $\sigma\omega$  term on the other hand. The total contribution is rather small, less than 1 MeV in absolute value, attractive and of long range. The small repulsion present at small separation distance is not significant and does not contribute to the binding energy because of the presence of correlations. It is important to note here that although the 3BF under consideration corresponds to the exchange of two heavy mesons (compared to the pion), it contributes mostly between 1 and 2 fm. Furthermore, since the potential is purely central, it contributes constructively in all partial waves, and therefore gives a rather large contribution to the binding energy per particle, as shown in Table III (about  $-4$  MeV at normal density). In addition, the contribution of the Roper resonance to the 3BF gives a correction to the potential energy in  $\rho_B^2$ . It dominates the correction from virtual  $N\bar{N}$  pair terms described in the preceding section at normal density, but is less important at higher density where the repulsive effect in  $\rho_B^{8/3}$  takes over. We indicate by a solid line in Fig. 9 the resulting equation of state once all corrections from the 3BF indicated in Fig. 3(a) and (b) have been taken into account. It is interesting to notice how the correction of  $-4$  MeV is influenced by the peculiarity of the vertex form factors. The specific orthogonality properties of the Roper wave function with respect to that of the nucleon induce a particular shape of the vertex form factor not predictable from qualitative arguments and at variance with monopole expressions commonly used. It is such as to reduce the energy per nucleon from the three-body force via the Roper by a factor of about 3 with respect to the one obtained with a pure monopole shape with identical asymptotic behavior at large momentum transfer. We view this result as indicating the importance of a consistent description of baryonic excitations at the quark level.

All the corrections discussed in this work are in fact equally important in bringing the saturation curve in qualitative agreement with the empirical results, starting from the simple calculation in terms of a two-body potential only (long-dashed line). Given the various approximations we made in treating the many-body problem and the derivation of the effective two-body potentials from the 3BF, as well as the model dependence of the parameters entering the contribution of the Roper resonance, we

believe that the small discrepancy which still persists is not very significant. It could only be settled through more tedious numerical works.

From a phenomenological point of view, the empirical equation of state constructed in Ref. 48 can easily be accounted for within our framework by giving a small density dependence to the  $\sigma$  mass. At small density,  $\rho < \rho_0/2$ , the corrections we analyzed in this work are very small, and therefore the equation of state is not sensitive to the mass of the  $\sigma$  meson. Between  $\rho_0/2$  and  $\rho_0$ , one needs extra attraction which can be achieved by lowering  $m_\sigma$  down to 450 MeV. On the other hand, at large density, the  $\sigma$  mass cannot be lowered that much (all other masses and coupling constant being kept fixed) in order to avoid saturation at too high density. It is interesting to note that the variation of  $m_\sigma$  we find is in qualitative agreement with the results of Ref. 30. The uncertainty in the medium dependence of the  $\sigma$ -meson mass is certainly a major limitation to a more precise evaluation of the 3BF contributions detailed in this work.

## VI. SUMMARY AND CONCLUSIONS

The basic observation underlying our study is twofold. On the one hand, it is the established capability of the nonrelativistic many-body theory of nucleons interacting via a two-body potential to give reliable results for nuclear matter and finite nuclei properties. On the other hand, it is the necessity to take into account in a consistent scheme the finite structure of the constituents and to evaluate corrections perturbatively. This is of utmost importance as the excited states of the nucleon enters significantly in the corrective processes. Suppressed degrees of freedom at the level of the two-body potential result in many body potentials, the three-body interactions coming first in the hierarchy. On a pure phenomenological basis, it has been shown<sup>24</sup> that an additional three-body potential is indeed capable to correct in a satisfactory way the many body results obtained from two-body forces only. However, the theoretical analysis of the corrective three-body interaction is quite involved, one major reason being that it cannot be disconnected in any way from the two-body potential one starts with. Hence, if one seeks a consistent description of the different interactions in the nuclear system, one cannot simply let various parameters of the residual forces evolve freely and take on values suited only for one purpose—empirical properties of nuclear matter and/or finite nuclei—and disregard other areas of physics where similar perturbative corrections have also been studied for long and mastered from comparison with a large body of data.

We have shown here that the actual knowledge of electromagnetic interactions in nuclei in terms of meson-exchange currents provides a link with well identified three-body processes. For a given two-body interaction, the constraints of current conservation and consistency with the one-boson exchange picture fixes all the model parameters which are not expected to depend much on the medium itself. This is the case of the masses, coupling constants, and form factors of well established mesons. The hypothetical scalar  $\sigma$  meson which provides



the intermediate-range attraction on a purely empirical basis in one-boson exchange models of the two-body interaction, has again a very specific role in the medium. Recent theoretical investigations have shown that medium corrections to the  $\sigma$  mass are strongly density dependent. Hence we have kept this mass as the only free parameter in the expression of the three-body forces resulting from our analysis of meson-exchange currents. In the first place, and to make the study of the three-body forces contributions to the nuclear matter binding energy simple, we fix  $m_\sigma$  at a given value (540 MeV) independent of density.

Although the calculation scheme we envisage to evaluate corrections is subject to limitations and amendable in many respects, we show that it incorporates correctly the dominant saturating effects brought about by the three-body forces. Hence we believe to have identified the characteristic trends in the saturation mechanism that are mostly independent of the technics of solution of the many-body problem itself. We find that these trends in modifying the equation of state from the two-body force only originate predominantly from two well identified processes. One relates to nucleon-antinucleon pair terms present in the analysis of meson-exchange currents. Its three-body counterpart gives a correction to the energy per particle which varies with a high power of the density and drives the system to lower density at saturation, stiffening the equation of state. The second one comes from subnucleonic degrees of freedom via the nucleon Roper resonance  $N^*(\frac{1}{2}, \frac{1}{2})$ . It counteracts the effect of the latter on the equation of state and drives it close to the empirical binding energy at normal saturation density. As the  $\pi$ - and  $\rho$ -exchange contributions from the Roper resonance are highly suppressed in first order in the three-body force because of their specific spin structures, the dominant role is played by processes with scalar and vector meson exchanges. This comes from the fact that the Roper, with the same quantum numbers as the nucleon, can easily couple spin with surrounding nucleons through a scalar (e.g., vector) interaction. However, quantitative results concerning the effect of the Roper in the nuclear medium have so far proved elusive due to a limited knowledge of coupling constants and form factors between meson-nucleon and this resonance. We have been able here to give a more quantitative answer through a determination of these quantities from a more realistic quark model in which the nucleon has a baglike structure.

The pending and most puzzling problem relates to the case of the hypothetical scalar meson. Our results clearly show the importance of the medium corrections to the

free  $\sigma$  mass in determining the equation of state. In fact we are now able to obtain rather easily a reasonable set of values of  $m_\sigma$  as a function of the density in order to reproduce a given empirical equation of state. However, due to the limitations of the calculations, we consider our numerical results for the density dependence as only indicative. Yet an important point we want to stress is the combined importance of both the strong repulsion from the pair terms and the attraction from the Roper terms in producing enough flexibility in the energy functional in terms of the  $\sigma$  mass to cope with the empirical situation. We achieve this goal here through consistent corrections to reasonably well controlled nuclear many-body results, in close connection to the successful analysis of meson-exchange currents in nuclei. This is in marked contrast to actual relativistic approaches of the nuclear many-body problem. Although successful in the mean-field description, they are presently out of control beyond this approximation and offer no possibility for the quark substructure of the constituents.

Future investigations of the effects of nucleon resonances and medium corrections to meson masses and coupling constants should hopefully bring our conclusion to a more quantitative basis. This is certainly possible, although not straightforward with existing and more elaborate techniques of solution of the many-body problem combined with a thorough description of meson and baryon properties from relativistic quark models.

#### ACKNOWLEDGMENTS

We would like to thank B. Desplanques, T. E. O. Ericson, and C. Gignoux for very fruitful discussion and J. Cugnon for a critical reading of the manuscript. One of us (J.-F.M.) gratefully acknowledges a fellowship from the CERN theory division where a large part of this work was done. The numerical calculations have been possible through allocation of computing time on IBM 3090 VF from the Fonds National de la Recherche Scientifique (Belgium). This work was supported in part by NATO Grant No. 025.81. The Division de Physique Theorique is a laboratory associated with CNRS.

#### APPENDIX A: COMPLETE EXPRESSIONS FOR THE $r$ -SPACE THREE-BODY FORCES FROM $2\omega$ AND $\sigma\omega$ EXCHANGE

The case of the  $2\sigma$ -exchange contribution is treated in Sec. IV A with the result  $W_3^{2\sigma}$  given in Eq. (31). We follow the same procedure here and give the expressions of  $W_3^{2\omega}$  and  $W_3^{\sigma\omega}$ . They write

$$\begin{aligned}
 W_3^{2\omega}(\mathbf{x}, \mathbf{y}; \mathbf{r}'_1, \mathbf{r}'_2 | \mathbf{r}_1, \mathbf{r}_2) &= \frac{g_{\omega N}^4}{4M^3} \frac{m_\omega^2}{(4\pi)^2} \delta^{(3)}(\mathbf{r}'_3 - \mathbf{r}_3) \\
 &\times \{ [(1 + \sigma_1 \cdot \sigma_2 + \sigma_1 \cdot \sigma_3 + \sigma_2 \cdot \sigma_3) \hat{\mathbf{x}} \cdot \hat{\mathbf{y}} - \sigma_1 \cdot \hat{\mathbf{y}} \sigma_3 \cdot \hat{\mathbf{x}} - \sigma_3 \cdot \hat{\mathbf{y}} \sigma_2 \cdot \hat{\mathbf{x}} - \sigma_1 \cdot \hat{\mathbf{y}} \sigma_2 \cdot \hat{\mathbf{x}}] Z'_\omega(x) Z'_\omega(y) \\
 &\quad + 2i Z'_\omega(y) Z_\omega(x) (\sigma_2 + \sigma_3) (\hat{\mathbf{y}} \times \nabla_{\mathbf{r}'_1}) + 2i Z'_\omega(x) Z_\omega(y) (\sigma_1 + \sigma_2) (\hat{\mathbf{x}} \times \nabla_{\mathbf{r}'_2}) \\
 &\quad - 4 Z_\omega(x) Z_\omega(y) \nabla_{\mathbf{r}'_1} \cdot \nabla_{\mathbf{r}'_2} \} \delta^{(3)}(\mathbf{r}'_2 - \mathbf{r}_2) \delta^{(3)}(\mathbf{r}'_1 - \mathbf{r}_1), \tag{A1}
 \end{aligned}$$

$$W_3^{\sigma\omega}(\mathbf{r}'_1, \mathbf{r}'_2, \mathbf{r}'_3 | \mathbf{r}_1, \mathbf{r}_2, \mathbf{r}_3) = \delta^{(3)}(\mathbf{r}'_1 - \mathbf{r}_1) W_{3,1}^{\sigma\omega}(\mathbf{x}, \mathbf{y}; \mathbf{r}'_2, \mathbf{r}'_3 | \mathbf{r}_2, \mathbf{r}_3) + \delta^{(3)}(\mathbf{r}'_2 - \mathbf{r}_2) W_{3,2}^{\sigma\omega}(\mathbf{x}, \mathbf{y}; \mathbf{r}'_1, \mathbf{r}'_3 | \mathbf{r}_1, \mathbf{r}_3), \quad (\text{A2})$$

with

$$W_{3,1}^{\sigma\omega}(\mathbf{x}, \mathbf{y}; \mathbf{r}'_2, \mathbf{r}'_3 | \mathbf{r}_2, \mathbf{r}_3) = \frac{g_{\sigma N}^2 g_{\omega N}^2}{4M^3} \frac{m_\omega m_\sigma}{(4\pi)^2} \left[ (1 + \sigma_2 \cdot \sigma_3) \left[ Z''_\omega(y) + \frac{2}{y} Z'_\omega(y) \right] Z_\sigma(x) \right. \\ - 2i Z_\sigma(x) Z'_\omega(y) (\sigma_2 + \sigma_3) \cdot (\hat{\mathbf{y}} \times \nabla_{\mathbf{r}'_3}) + i Z'_\sigma(x) Z'_\omega(y) (\sigma_2 + \sigma_3) \cdot (\hat{\mathbf{x}} \times \hat{\mathbf{y}}) \\ + 2i Z_\sigma(x) Z'_\omega(y) \sigma_3 \cdot (\hat{\mathbf{y}} \times \nabla_{\mathbf{r}'_2}) + 2Z'_\sigma(x) Z_\omega(y) \hat{\mathbf{x}} \cdot \nabla_{\mathbf{r}'_2} + 2Z_\sigma(x) Z'_\omega(y) \hat{\mathbf{y}} \cdot \nabla_{\mathbf{r}'_2} \\ \left. + 4Z_\sigma(x) Z_\omega(y) \nabla_{\mathbf{r}'_2} \cdot \nabla_{\mathbf{r}'_3} - \frac{1}{3} (\sigma_2 \cdot \sigma_3 Y_2^\omega(y) + S_{23}(\hat{\mathbf{y}}) X_2^\omega(y)) Z_\sigma(x) \right] \\ \times \delta^{(3)}(\mathbf{r}'_3 - \mathbf{r}_3) \delta^{(3)}(\mathbf{r}'_2 - \mathbf{r}_2), \quad (\text{A3})$$

and  $W_{3,2}^{\sigma\omega}$  obtained from  $W_{3,1}^{\sigma\omega}$  with the interchanges

$$\{\sigma_1 \rightleftharpoons \sigma_2, \mathbf{r}'_1 \rightleftharpoons \mathbf{r}'_2, \mathbf{r}_1 \rightleftharpoons \mathbf{r}_2, x \rightleftharpoons y\}.$$

In these expressions  $Z_{\sigma(\omega)}(x)$  is defined in Eq. (32) and  $Y_2^\omega(x), X_2^\omega(x)$  are given in Eq. (2.24) of Ref. 18 with  $\mathbf{x} = \mathbf{r}'_3 - \mathbf{r}'_1$  and  $\mathbf{y} = \mathbf{r}'_3 - \mathbf{r}'_2$ .

In the derivation of the effective two-body force, according to the general expression (29), we note that by tracing over the spin (isospin) of the third particle all terms linear in  $\sigma_3(\tau_3)$  drop out. Likewise, terms in  $\hat{\mathbf{x}} \times \hat{\mathbf{y}}, \hat{\mathbf{y}} \times \nabla_{\mathbf{r}'_1}, \hat{\mathbf{x}} \times \nabla_{\mathbf{r}'_1}$  do not contribute after integration and in keeping with the derivation of the  $(\pi, \rho)$  contribution of Ref. 18, the overall potential  $V_3$  is kept local in the variables  $(\mathbf{r}_1, \mathbf{r}_2)$ , with  $\mathbf{r} = \mathbf{r}_1 - \mathbf{r}_2$ .

The part  $V_3^{2\sigma,2}$  completing the expression given in (33b) writes

$$V_3^{2\sigma,2}(r) = -\frac{g_{\sigma N}^2}{4M^3} \frac{m_\sigma^2}{(4\pi)^2} \rho_B \int d^3 r_3 g(x) g(y) \left\{ \left[ 4g'(x)g(y) [Z'_\sigma(x)Z_\sigma(y) + \hat{\mathbf{x}} \cdot \hat{\mathbf{y}} Z_\sigma(x)Z'_\sigma(y)] \right. \right. \\ \left. \left. + g(x)g(y) \left[ Z''_\sigma(x) + \frac{2}{x} Z'_\sigma(x) \right] Z_\sigma(y) + x \rightleftharpoons y \right] \right. \\ \left. + \hat{\mathbf{x}} \cdot \hat{\mathbf{y}} g(x)g(y) Z'_\sigma(x)Z'_\sigma(y) \right\}. \quad (\text{A4})$$

From Eq. (A1) the effective force  $V_3^{2\omega}(r)$  writes

$$V_3^{2\omega}(\mathbf{r}) = V_{3,C}^{2\omega}(r) + \sigma_1 \cdot \sigma_2 V_{3,\sigma}^{2\omega}(r) + S_{12}(\hat{\mathbf{r}}) V_{3,T}^{2\omega}(r), \quad (\text{A5})$$

with

$$V_{3,C}^{2\omega}(r) = \frac{g_{\omega N}^4}{4M^3} \frac{m_\omega^2}{(4\pi)^2} \rho_B \int d^3 r_3 g^2(x) g^2(y) \hat{\mathbf{x}} \cdot \hat{\mathbf{y}} Z'_\omega(x) \\ \times Z'_\omega(y), \quad (\text{A6})$$

$$V_{3,\sigma}^{2\omega}(r) = \frac{2}{3} V_{3,C}^{2\omega}(r), \quad (\text{A7})$$

$$V_{3,T}^{2\omega}(r) = -\frac{g_{\omega N}^4}{4M^3} \frac{m_\omega^2}{(4\pi)^2} \rho_B \int d^3 r_3 g^2(x) g^2(y) \frac{1}{3} Q Z'_\omega(x) \\ \times Z'_\omega(y). \quad (\text{A8})$$

Here  $Q = -\frac{1}{2}(\cos\theta + 3\cos\theta_x \cos\theta_y)$ ,  $\cos\theta = \hat{\mathbf{x}} \cdot \hat{\mathbf{y}} = (x^2 + y^2 - r^2)/2xy$ ,  $\cos\theta_x = (y^2 - x^2 - r^2)/2xr$ , and  $\cos\theta_y = (x^2 - y^2 - r^2)/2yr$ .

From the sum  $W_{3,1}^{\sigma\omega} + W_{3,2}^{\sigma\omega}$  we obtain only a central effective force  $V_3^{\sigma\omega}(r)$  which writes

$$V_3^{\sigma\omega}(r) = \frac{g_{\sigma N}^2 g_{\omega N}^2}{4M^3} \frac{m_\omega m_\sigma}{(4\pi)^2} \rho_B \int d^3 r_3 g^2(x) g^2(y) \\ \times \left[ \left[ Z''_\omega(y) + \frac{2}{y} Z'_\omega(y) \right] Z_\sigma(x) + x \rightleftharpoons y \right]. \quad (\text{A9})$$

Here the functions  $Z_{\sigma(\omega)}(x)$  and derivatives are obtained from Eq. (32) and  $\int d^3 r_3$  is explicitated after Eq. (33b).

## APPENDIX B: MOMENTUM-SPACE THREE-BODY FORCES FROM $\sigma$ AND $\omega$ EXCHANGE VIA THE ROPER RESONANCE, AND CORRESPONDING EFFECTIVE TWO-BODY POTENTIALS

The relevant diagrammatic contributions are represented in Fig. 3. We use the notation of Secs. III B and V, and denote by  $M_R$  the Roper mass,  $\delta = M/M_R$  and  $F_\sigma^R(q^2)$  the  $\sigma$ -Roper form factor. For the order in momentum over the nucleon mass, consistent with the derivation of expressions (21), the  $2\sigma$ -Roper three-body force in momentum space writes

$$\begin{aligned}
\langle \mathbf{p}'_1, \mathbf{p}'_2, \mathbf{p}'_3 | W_3^{2\sigma-R} | \mathbf{p}_1, \mathbf{p}_2, \mathbf{p}_3 \rangle &= -(2\pi)^3 \delta^{(3)}(\mathbf{p}'_3 - \mathbf{p}_3 - \mathbf{q}_1 - \mathbf{q}_2) \cdot \frac{g_{\sigma N}^2 g_{\sigma R}^2}{M_R(1-\delta)} \frac{F_\sigma(q_1^2) F_\sigma^R(q_1^2)}{q_1^2 + m_\sigma^2} \frac{F_\sigma(q_2^2) F_\sigma^R(q_2^2)}{q_2^2 + m_\sigma^2} \\
&\times 2 \left[ 1 + \frac{\mathbf{p}_3^2}{4M^2} (1-\delta^2) + \frac{\mathbf{p}_3 \cdot (\mathbf{q}_1 + \mathbf{q}_2)}{4M^2} \left[ 1 - \delta^2 - \frac{2\delta}{(1-\delta)} \right] \right. \\
&\quad + \frac{(\mathbf{q}_1^2 + \mathbf{q}_2^2)}{4M^2} \left[ 1 - \frac{1}{2}\delta - \frac{1}{2}\delta^2 - \frac{\delta^2}{(1-\delta)} \right] + \frac{\mathbf{q}_1 \cdot \mathbf{q}_2}{4M^2} (1-\delta) \\
&\quad \left. + \frac{i}{4MM_R} \sigma_3 \cdot \mathbf{p}_3 \times (\mathbf{q}_1 + \mathbf{q}_2) - \frac{i}{4M^2} \sigma_1 \cdot (\mathbf{p}'_1 \times \mathbf{p}_1) - \frac{i}{4M^2} \sigma_2 \cdot (\mathbf{p}'_2 \times \mathbf{p}_2) \right]. \quad (\text{B1})
\end{aligned}$$

In the case of  $2\omega$  and  $\sigma\omega$  exchanges, we distinguish between the scalar  $F_\omega^{R,S}(q^2)$  and vector  $F_\omega^{R,V}(q^2)$   $\omega$ -Roper form factors. In the effective two-body potential approach only terms involving the scalar part contribute. For completeness, the full expressions of the  $2\omega$ - and  $\sigma\omega$ -Roper three-body forces in momentum space, obtained to the same order in the expansion as for (B1) are given. They write

$$\begin{aligned}
\langle \mathbf{p}'_1, \mathbf{p}'_2, \mathbf{p}'_3 | W_3^{2\omega-R} | \mathbf{p}_1, \mathbf{p}_2, \mathbf{p}_3 \rangle &= -(2\pi)^3 \delta^{(3)}(\mathbf{p}'_3 - \mathbf{p}_3 - \mathbf{q}_1 - \mathbf{q}_2) \cdot \frac{g_{\omega N}^2 g_{\omega R}^2}{2M_R^2(1-\delta)} \frac{F_\omega(q_1^2) F_\omega^R(q_2^2)}{(q_1^2 + m_\omega^2)(q_2^2 + m_\omega^2)} \\
&\times \left\{ 4M_R F_\omega^{R,S}(q_1^2) F_\omega^{R,S}(q_2^2) \left[ 1 + \frac{\mathbf{p}_3^2}{4M^2} (1+4\delta-\delta^2) + \frac{\mathbf{p}_3 \cdot (\mathbf{q}_1 + \mathbf{q}_2)}{4M^2} \left[ 1 - \frac{2\delta}{1-\delta} + 4\delta - \delta^2 \right] \right. \right. \\
&\quad + \frac{(\mathbf{q}_1^2 + \mathbf{q}_2^2)}{8M^2} \left[ 1 + \delta - \delta^2 - \frac{2\delta^2}{(1-\delta)} \right] + \frac{\mathbf{q}_1 \cdot \mathbf{q}_2}{4M^2} (1+\delta) \\
&\quad + \frac{\mathbf{p}_1^2}{2M^2} + \frac{\mathbf{p}_2^2}{2M^2} + \frac{i}{4M^2} \sigma_1 \cdot (\mathbf{p}'_1 \times \mathbf{p}_1) \\
&\quad \left. + \frac{i}{4M^2} \sigma_2 \cdot (\mathbf{p}'_2 \times \mathbf{p}_2) - \frac{i}{4MM_R} \sigma_3 \cdot [\mathbf{p}_3 \times (\mathbf{q}_1 + \mathbf{q}_2)] \right\} \\
&- \frac{1}{2M\delta} F_\omega^{R,S}(q_1^2) F_\omega^{R,V}(q_2^2) [(1+\delta)(2\mathbf{p}_3 + \mathbf{q}_1 + \mathbf{q}_2) - i(1-\delta)(\sigma_3 \times \mathbf{q}_1) + i(1+\delta)(\sigma_3 \times \mathbf{q}_2)] \\
&\times (2\mathbf{P} - i\sigma_2 \times \mathbf{q}_2) - \frac{1}{2M\delta} F_\omega^{R,V}(q_1^2) F_\omega^{R,S}(q_2^2) \\
&\times [(1+\delta)(2\mathbf{p}_3 + \mathbf{q}_1 + \mathbf{q}_2) - i(1-\delta)(\sigma_3 \times \mathbf{q}_2) + i(1+\delta)(\sigma_3 \times \mathbf{q}_1)] (2\mathbf{P}_1 - i\sigma_1 \times \mathbf{q}_1) \Big\}. \quad (\text{B2})
\end{aligned}$$

and

$$\begin{aligned}
\langle \mathbf{p}'_1, \mathbf{p}'_2, \mathbf{p}'_3 | W_3^{\sigma\omega-R} | \mathbf{p}_1, \mathbf{p}_2, \mathbf{p}_3 \rangle &= (2\pi)^3 \delta^{(3)}(\mathbf{p}'_3 - \mathbf{p}_3 - \mathbf{q}_1 - \mathbf{q}_2) \frac{g_{\omega N} g_{\omega R} g_{\sigma N} g_{\sigma R}}{2M_R^2(1-\delta)} \\
&\times \left[ \frac{F_\sigma(q_1^2) F_\sigma^R(q_1^2) F_\omega(q_2^2)}{(q_1^2 + m_\sigma^2)(q_2^2 + m_\omega^2)} \left\{ 4F_\omega^{R,S}(q_2^2) M_R \left[ 1 + \frac{\mathbf{p}_3^2}{4M^2} (1+3\delta-\delta^2) + \frac{\mathbf{p}_3 \cdot \mathbf{q}_1}{4M^2} \left[ 1+2\delta-2\delta^2 - \frac{4\delta^2}{1-\delta} \right] \right. \right. \right. \\
&\quad + \frac{\mathbf{p}_3 \cdot \mathbf{q}_2}{4M^2} (1+\delta) + \frac{\mathbf{q}_1^2}{4M^2} \left[ 1+\delta-\delta^2 - \frac{2\delta^2}{1-\delta} \right] \\
&\quad + \frac{\mathbf{q}_2^2}{8M^2} + \frac{\mathbf{q}_1 \cdot \mathbf{q}_2}{4M^2} (1+\delta) + \frac{\mathbf{p}_2^2}{2M^2} + \frac{i}{4MM_R} \sigma_3 \cdot (\mathbf{q}_2 \times \mathbf{p}_3) \\
&\quad \left. - \frac{i}{4M^2} \sigma_1 \cdot (\mathbf{p}'_1 \times \mathbf{p}_1) + \frac{i}{4M^2} \sigma_3 \cdot (\mathbf{p}'_2 \times \mathbf{p}_2) \right\} \\
&- \frac{1}{2M\delta} F_\omega^{R,V}(q_2^2) [(1+\delta)(2\mathbf{p}_3 + \mathbf{q}_1 + \mathbf{q}_2) - i(1-\delta)(\sigma_3 \times \mathbf{q}_1) \\
&\quad + i(1+\delta)(\sigma_3 \times \mathbf{q}_2)] (2\mathbf{P}_2 - i\sigma_2 \times \mathbf{q}_2) \Big\} + 1 \leftrightarrow 2 \Big] \quad (\text{B3})
\end{aligned}$$

TABLE IV. Coefficients of Eq. (B4).

$\alpha$	$C^{\alpha-R}$	$I_1^{\alpha-R}$	$I_2^{\alpha-R}$	$I_3^{\alpha-R}$	$I_4^{\alpha-R}$	$I_5^{\alpha-R}$
$2\sigma$	$\frac{g_{\sigma N}^2 g_{\sigma R}^2}{M_R} \left[ \frac{m_\sigma}{4\pi} \right]^2$	$-\frac{2}{(1-\delta)}$	$-\frac{(1+\delta)}{2}$	$\frac{1}{2} \left[ 1 + \delta - \frac{2\delta}{(1-\delta)^2} \right]$	$\frac{\left[ 1 - \frac{\delta}{2} - \frac{\delta^2}{2} - \frac{\delta^2}{1-\delta} \right]}{2(1-\delta)}$	$\frac{1}{2}$
$2\omega$	$\frac{g_{\omega N}^2 g_{\omega R}^2}{M_R} \left[ \frac{m_\omega}{4\pi} \right]^2$	$-\frac{2}{(1-\delta)}$	$-\frac{(1+4\delta-\delta^2)}{2(1-\delta)}$	$\frac{\left[ 1 + 4\delta - \delta^2 - \frac{2\delta}{(1-\delta)} \right]}{2(1-\delta)}$	$\frac{\left[ 1 + \delta - \delta^2 - \frac{2\delta^2}{1-\delta} \right]}{4(1-\delta)}$	$\frac{(1+\delta)}{2(1-\delta)}$
$\sigma\omega$	$\frac{g_{\omega N} g_{\omega R} g_{\sigma N} g_{\sigma R}}{M_R} \frac{m_\omega m_\sigma}{(4\pi)^2}$	$\frac{2}{(1-\delta)}$	$\frac{(1+3\delta-\delta^2)}{2(1-\delta)}$	$\frac{-1}{2(1-\delta)}$	$\frac{-1}{2(1-\delta)}$	$-\frac{(1+\delta)}{2(1-\delta)}$

Specifying the form factors (cf. Secs. III B and V), the  $r$ -space expressions of these contributions can be obtained in a straightforward though cumbersome way. We do not use them directly in our calculations, hence we only give the expressions of the local two-body effective forces  $V_3$  defined in Eq. (29) and derived from Eqs. (B1) to (B3). They write, for  $\alpha$  taken successively as  $2\sigma$ ,  $2\omega$ , and  $\sigma\omega$

$$V_3^{\alpha-R}(r) = C^{\alpha-R} \sum_{i=1}^5 I_i^{\alpha-R} V_{3,i}^{\alpha-R}. \quad (\text{B4})$$

with the coefficients  $C^{\alpha-R}$  and  $I_i^{\alpha-R}$  given in Table IV and the following functions  $V_{3,i}^{\alpha-R}(r)$

(i)  $\alpha$  taken as  $2\sigma$  or  $2\omega$

$$V_{3,1}^{\alpha-R}(r) = \rho_B \int d^3 r_3 g^2(x) g^2(y) Z_\alpha^R(x) Z_\alpha^R(y), \quad (\text{B5a})$$

$$V_{3,2}^{\alpha-R}(r) = M^{-2} \rho_B \left[ \frac{3}{5} \left[ \frac{3\pi^2}{2} \rho_B \right]^{2/3} \int d^3 r_3 g^2(x) g^2(y) Z_\alpha^R(x) Z_\alpha^R(y) + \int d^3 r_3 [g(y) Z_\alpha^R(y) (g(y) g'(x) + \hat{x} \cdot \hat{y} g(x) g'(y)) (g'(x) Z_\alpha^R(x) + Z_\alpha^{R'}(x) g(x)) + x \rightleftharpoons y] \right], \quad (\text{B5b})$$

$$V_{3,3}^{\alpha-R}(r) = M^{-2} \rho_B \int d^3 r_3 g(x) g(y) [(Z_\alpha^{R'}(x) Z_\alpha^R(y) + \hat{x} \cdot \hat{y} Z_\alpha^R(x) Z_\alpha^{R'}(y)) g'(x) g(y) + x \rightleftharpoons y], \quad (\text{B5c})$$

$$V_{3,4}^{\alpha-R}(r) = M^{-2} \rho_B \int d^3 r_3 g^2(x) g^2(y) \left[ \left[ Z_\alpha^{R''}(x) + \frac{2}{x} Z_\alpha^{R'}(x) \right] Z_\alpha^R(y) + x \rightleftharpoons y \right], \quad (\text{B5d})$$

$$V_{3,5}^{\alpha-R}(r) = M^{-2} \rho_B \int d^3 r_3 \hat{x} \cdot \hat{y} Z_\alpha^{R'}(x) Z_\alpha^{R'}(y). \quad (\text{B5e})$$

Here the function  $Z_\alpha^R(x)$  and derivatives are obtained in closed form

$$Z_\alpha^R(x) = \left[ \frac{4\pi}{m_\alpha} \right] \int \frac{d^3 q}{(2\pi)^3} \frac{e^{iq \cdot x}}{(q^2 + m_\alpha^2)} F_\alpha(q^2) F_\alpha^R(q^2), \quad (\text{B6})$$

with the form factors  $F_\alpha(q^2)$  from Eq. (5) with parameters of Table I, and  $F_\alpha^R(q^2)$  from Eq. (44) with parameters given in Sec. V.

(ii)  $\alpha$  taken as  $\sigma\omega$

$$V_{3,1}^{\sigma\omega-R}(r) = \rho_B \int d^3 r_3 g^2(x) g^2(y) (Z_\alpha^R(x) Z_\omega^R(y) + x \rightleftharpoons y), \quad (\text{B7a})$$

$$V_{3,2}^{\sigma\omega-R}(r) = M^{-2} \rho_B \left[ \frac{3}{5} \left[ \frac{3\pi^2}{2} \rho_B \right]^{2/3} \int d^3 r_3 g^2(x) g^2(y) (Z_\sigma^R(x) Z_\omega^R(y) + x \rightleftharpoons y) + \int d^3 r_3 [g(y) Z_\omega^R(y) (g(y) g'(x) + \hat{x} \cdot \hat{y} g(x) g'(y)) (g'(x) Z_\sigma^R(x) + Z_\sigma^{R'}(x) g(x)) + x \rightleftharpoons y + g(y) Z_\sigma^R(y) (g(y) g'(x) + \hat{x} \cdot \hat{y} g(x) g'(y)) (g'(x) Z_\omega^R(x) + Z_\omega^{R'}(x) g(x)) + x \rightleftharpoons y] \right], \quad (\text{B7b})$$

$$V_{3,3}^{\sigma\omega-R}(r) = M^{-2}\rho_B \left\{ \left[ 1 + 2\delta - 2\delta^2 - 4\frac{\delta^2}{1-\delta} \right] \int d^3r_3 g(x)g(y) [Z_\sigma^{R'}(x)Z_\omega^R(y)(g'(x)g(y) + \hat{x}\cdot\hat{y}g(x)g'(y)) + x \rightleftharpoons y] \right. \\ \left. + (1+\delta) \int d^3r_3 g(x)g(y) [Z_\omega^R(x)Z_\sigma^R(y)(g'(x)g(y) + \hat{x}\cdot\hat{y}g(x)g'(y)) + x \rightleftharpoons y] \right\}, \quad (\text{B7c})$$

$$V_{3,4}^{\sigma\omega-R}(r) = M^{-2}\rho_B \left\{ \left[ 1 + \delta - \delta^2 - 2\frac{\delta^2}{1-\delta} \right] \int d^3r_3 g^2(x)g^2(y) \left[ Z_\omega^R(x) \left[ Z_\sigma^{R''}(y) + \frac{2}{y}Z_\sigma^{R'}(y) \right] + x \rightleftharpoons y \right] \right. \\ \left. + \frac{1}{2} \int d^3r_3 g^2(x)g^2(y) \left[ Z_\sigma^R(x) \left[ Z_\omega^{R''}(y) + \frac{2}{y}Z_\omega^{R'}(y) \right] + x \rightleftharpoons y \right] \right\}, \quad (\text{B7d})$$

$$V_{3,5}^{\sigma\omega-R}(r) = M^{-2}\rho_B \int d^3r_3 g^2(x)g^2(y) \hat{x}\cdot\hat{y} (Z_\sigma^{R'}(x)Z_\omega^R(y) + x \rightleftharpoons y). \quad (\text{B7e})$$

- <sup>1</sup>R. Brockmann and W. Weise, Phys. Rev. C **16**, 1282 (1977); L. D. Miller and A. E. S. Green, Phys. Rev. C **5**, 241 (1972).
- <sup>2</sup>B. C. Clark, S. Hama, R. L. Mercer, L. Ray, and B. D. Serot, Phys. Rev. Lett. **50**, 1644 (1983); B. C. Clark, R. L. Mercer, and P. Schwandt, Phys. Lett. **122B**, 211 (1983).
- <sup>3</sup>A. D. Jackson, Ann. Rev. Nucl. Part. Sci. **33**, 105 (1983).
- <sup>4</sup>B. D. Day, Rev. Mod. Phys. **50**, 495 (1978); B. D. Day and R. B. Wiringa, Phys. Rev. C **32**, 1057 (1985).
- <sup>5</sup>I. E. Lagaris and V. R. Pandharipande, Nucl. Phys. **A359**, 331 (1981); **A359**, 349 (1981).
- <sup>6</sup>J. D. Walecka, Ann. Phys. (N.Y.) **83**, 491 (1974); B. D. Serot and J. D. Walecka, Adv. Nucl. Phys. **16** (1985).
- <sup>7</sup>M. R. Anastasio, L. S. Celenza, W. S. Pong, and C. M. Shakin, Phys. Rep. **100**, 1 (1983).
- <sup>8</sup>C. J. Horowitz and B. D. Serot, Nucl. Phys. **A464**, 613 (1987).
- <sup>9</sup>B. Ter Haar and R. Malfiet, Phys. Rep. **149**, 207 (1987).
- <sup>10</sup>R. Brockmann and R. Machleidt, Phys. Lett. **149B**, 283 (1984).
- <sup>11</sup>G. E. Brown, W. Weise, G. Baym, and J. Speth, Comments Nucl. Part. Phys. **17**, 39 (1987); T. L. Ainsworth, E. Baron, G. E. Brown, L. Cooperstein, and M. Prakash, Nucl. Phys. **A464**, 740 (1987).
- <sup>12</sup>J. W. Negele, Comments Nucl. Part. Phys. **14**, 303 (1985).
- <sup>13</sup>I. Zahed, Phys. Rev. C **37**, 409 (1988).
- <sup>14</sup>J.-F. Mathiot, Phys. Rep. **173**, 63 (1989), and references therein.
- <sup>15</sup>D. Schütte, Nucl. Phys. **A411**, 369 (1983).
- <sup>16</sup>A. Hosaka and H. Toki, Int. J. Mod. Phys. **A3**, 1413 (1988).
- <sup>17</sup>S. A. Coon, M. D. Scadron, P. C. McNamee, B. R. Barret, D. W. E. Blatt, and B. H. J. McKellar, Nucl. Phys. **A317**, 242 (1979).
- <sup>18</sup>R. G. Ellis, S. A. Coon, and B. H. J. McKellar, Nucl. Phys. **A438**, 631 (1985).
- <sup>19</sup>P. Grangé, M. Martzolff, Y. Nogami, D. W. L. Sprung, and C. K. Ross, Phys. Lett. **60B**, 237 (1976); P. Grangé and M. Martzolff, Lett. Nuovo Cimento **16**, 15 (1976); M. Martzolff, B. Loiseau, and P. Grangé, Phys. Lett. **92B**, 46 (1980).
- <sup>20</sup>B. Loiseau, Y. Nogami, and C. K. Ross, Nucl. Phys. **A165**, 601 (1971).
- <sup>21</sup>H. T. Coelho, T. K. Das, and M. R. Robilotta, Phys. Rev. C **28**, 1812 (1983); M. R. Robilotta and H. T. Coelho, Nucl. Phys. **A460**, 645 (1986).
- <sup>22</sup>B. D. Keister and R. B. Wiringa, Phys. Lett. **B173**, 5 (1986).
- <sup>23</sup>M. Lacombe, B. Loiseau, J. M. Richard, R. Vinh Mau, J. Coté, and R. de Tourreil, Phys. Rev. C **21**, 861 (1980).
- <sup>24</sup>J. Carlson, W. R. Pandharipande, and R. B. Wiringa, Nucl. Phys. **A401**, 59 (1983).
- <sup>25</sup>A. Lejeune, P. Grangé, M. Martzolff, and J. Cugnon, Nucl. Phys. **A453**, 189 (1986).
- <sup>26</sup>B. H. J. McKellar and R. Rajamaran, Phys. Rev. C **3**, 1877 (1971); in *Mesons in Nuclei*, edited by M. Rho and D. Wilkinson (North-Holland, Amsterdam, 1979), p. 357.
- <sup>27</sup>H. B. Nielsen and A. Patkos, Nucl. Phys. **B195**, 137 (1982); G. Mack, *ibid.* **B235**, 137 (1984); H. J. Pirner, J. Wroldsen, and M. Ilgenfritz, *ibid.* **B294**, 905 (1987).
- <sup>28</sup>D. O. Riska, Phys. Scripta **31**, 107 (1985).
- <sup>29</sup>G. E. Brown, Prog. Theor. Phys. **91**, 85 (1987).
- <sup>30</sup>V. Bernard, U. G. Meissner, and I. Zahed, Phys. Rev. Lett. **59**, 966 (1987).
- <sup>31</sup>R. Machleidt, K. Holinde, and Ch. Elster, Phys. Rep. **149**, 1 (1987).
- <sup>32</sup>A. Bouyssy, J.-F. Mathiot, Nguyen Van Giai, and S. Marcos, Phys. Rev. C **36**, 380 (1987).
- <sup>33</sup>B. Fridman and V. R. Pandharipande, Nucl. Phys. **A361**, 502 (1981).
- <sup>34</sup>T. T. S. Kuo, Z. Y. Ma, and R. Vinh Mau, Phys. Rev. C **33**, 717 (1986).
- <sup>35</sup>J. Torre, J. J. Benayoun, and J. Chauvin, Z. Phys. **A300**, 319 (1981); T. Sasakawa and S. Ishikawa, Few Body System **1**, 3 (1986); J. L. Friar, B. F. Gibson, and G. L. Payne, Los Alamos Report LA-UR, 88-96.
- <sup>36</sup>G. Cory, M. Dufresne, C. Gignoux, G. Goulard, P. Grangé, and J.-F. Mathiot (unpublished).
- <sup>37</sup>B. D. Day, Phys. Rev. **151**, 826 (1966).
- <sup>38</sup>J.-P. Jeukenne, A. Lejeune, and C. Mahaux, Phys. Rep. **25C**, 85 (1976).
- <sup>39</sup>C. Mahaux, P. F. Bortignon, R. A. Broglia, and C. H. Dasso, Phys. Rep. **120C**, 1 (1985).
- <sup>40</sup>V. Bernard, thèse de doctorat és Sciences, Strasbourg, 1986.
- <sup>41</sup>B. Desplanques, Z. Phys. **A330**, 331 (1988).
- <sup>42</sup>K. Shimizu, A. Polls, H. Mütter, and A. Faessler, Nucl. Phys. **A364**, 461 (1981).
- <sup>43</sup>Particle Data Group, Review of particles properties, April 1984.
- <sup>44</sup>H. R. Fiebig and B. Schwesinger, Nucl. Phys. **A393**, 349 (1983); F. Myhrer and J. Wroldsen, Z. Phys. **25C**, 281 (1985).
- <sup>45</sup>G. E. Brown, J. D. Durso, and M. Johnson, Nucl. Phys. **A397**, 447 (1984).
- <sup>46</sup>P. Guichon, Phys. Lett. **164B**, 361 (1985).
- <sup>47</sup>J.-F. Mathiot, G. Chanfray, and H. J. Pirner (unpublished).
- <sup>48</sup>D. W. L. Sprung and P. K. Banerjee, Nucl. Phys. **A168**, 273 (1971).